NACA RM E55I15

NACA

RESEARCH MEMORANDUM

BOUNDARY-LAYER TRANSITION AT HIGH REYNOLDS NUMBERS AS OBTAINED IN FLIGHT OF A 20° CONE-CYLINDER WITH WALL TO LOCAL STREAM TEMPERATURE RATIOS NEAR 1.0

By Leonard Rabb and John H. Disher

Lewis Flight Propulsion Laboratory
Cleveland, Ohio

NATIONAL ADVISORY COMMITTEE FOR AERONAUTICS

WASHINGTON
November 3, 1955
Declassified February 8, 1960

NATIONAL ADVISORY COMMITTEE FOR AERONAUTICS

RESEARCH MEMORANDUM

BOUNDARY-LAYER TRANSITION AT HIGH REYNOLDS NUMBERS AS OBTAINED IN FLIGHT OF A 20° CONE-CYLINDER WITH WALL TO LOCAL STREAM TEMPERATURE RATIOS NEAR 1.0

By Leonard Rabb and John H. Disher

SUMMARY

A highly polished 20° included-angle cone-cylinder body of revolution has been flown to obtain heat-transfer and boundary-layer-transition data at low ratios of wall to local stream temperature. During the flight, a maximum free-stream Mach number of 5.02 and a maximum local Reynolds number on the conical surface of 50×10^6 were reached. Transitions from a turbulent to a laminar and from a laminar to a turbulent boundary layer were observed at each of seven measuring stations on the cone. The maximum local Reynolds number at which laminar flow was observed was 32×10^6.

Van Driest's analysis of boundary-layer stability at infinite Reynolds numbers for local Mach numbers from 2.5 to 4.0 closely approximates the conditions under which transition occurred during this investigation when the analysis is based on a Prandtl number of 1.0 and a linear relation of viscosity with temperature. A recent analysis by Dunn and Lin of stability criteria for three-dimensional disturbances for a Prandtl number of 0.75 agrees more closely with the flight data at a Mach number of 4.0 than does Van Driest's two-dimensional solution for the same Prandtl number and viscosity assumptions.

INTRODUCTION

The design of hypersonic ballistic missiles can depend critically on the type of boundary layer that exists along the body. If laminar flow can be maintained over the major portion of the exposed missile surface area, the heat transfer into the body during re-entry will be only a fraction of that for a turbulent boundary layer, and appreciable economies in missile weight and cost can be effected.

Analyses (refs. 1 and 2) have indicated that at supersonic Mach numbers, laminar boundary layers can be maintained to high Reynolds numbers by properly cooling the skin of the vehicle. However, these analyses, although qualitatively substantiated (refs. 3 and 4), do not account for the effects of such variables as free-stream turbulence, surface roughness, and shock waves or other external disturbances. Experimental data are needed for evaluating theory and for practical application to missile design.

Because of the high Reynolds numbers and stagnation temperatures involved, and because of the unknown effect of wind-tunnel-induced turbulence, free-flight tests are at present the only means for obtaining much of the desired information. In addition to needs for evaluation of boundary-layer stability criteria, data are needed on heat-transfer coefficients at high Mach numbers and Reynolds numbers. To facilitate publication of the data, this report will present only the data concerning boundary-layer stability.

The data reported herein were obtained from the flight of an air-launched rocket-propelled cone-cylinder body of revolution that was designed to obtain boundary-layer-stability and heat-transfer information for a 20° included-angle cone at free-stream Mach numbers up to approximately 5.0. During the accelerating part of the flight, the ratio of skin temperature to local stream static temperature remained within a region where theoretically the laminar boundary layer would be completely stable to two-dimensional disturbances.

APPARATUS AND PROCEDURE

A sketch of the model giving pertinent dimensions is shown in figure 1 and a photograph of the 20° included-angle nose cone is shown in figure 2.

A complete general description of the type of model used, the instrumentation, and the calculation procedure is given in references 5, 6, and 7. The model described herein differed from those of references 5 and 6 as follows: (1) Gross weight at launching was reduced to 197 pounds by reducing the weight of lead ballast in the nose from 13.5 to 8 pounds; (2) The telemeter antenna was moved from the nose cone to the trailing edge of the fins (fig. 3) in order to allow a continuously smooth cone surface; (3) The surface finish of the cone was $1\frac{1}{2}$ to 2 micro inch rms as determined by a Brush surface analyzer. This degree of finish was obtained by a metallurgical polishing technique using progressively finer grades of diamond polishing compound.

The instrumentation consisted of two axial accelerometers and nine resistance-wire skin-temperature elements. Of the nine temperature elements, two failed prior to launching.

The locations of the seven usable temperature elements are shown in figure 4. Six of the elements were located in a line at slant distances of 11.66, 14.16, 18.28, 20.97, 23.53, and 25.84 inches from the cone apex. The seventh element was located at the 23.53-inch station on the opposite side of the cone ($\theta = 180^{\circ}$). The skin thickness at the temperature-element locations ranged from 0.0295 to 0.0321 inch. The two accelerometers covered ranges of -2 to +37 and 0 to -12 gravitational units, respectively, and were connected to a common telemeter channel. The range was switched from positive to negative during flight by the "g" switch shown in figure 5.

The model was released at a high altitude from an F82 airplane and was propelled by a solid propellant 6KS3000 rocket housed within the cylindrical portion of the vehicle.

The calculation procedure was similar to that described in reference 6 except as altered by the fact that static and total pressures were not measured during this flight. Therefore, the free-stream velocity was obtained by integrating acceleration data and from radar tracking. The free-stream static pressure was obtained from the calculated altitude and an atmospheric survey conducted by the carrier airplane following the missile flight.

RESULTS AND DISCUSSION

Time histories of free-stream velocity, free-stream Mach number, axial acceleration, free-stream and cone Reynolds number per foot, and free-stream static pressure are presented in figure 6. A curve of altitude against horizontal range is plotted in figure 7. The model was launched at an altitude of 35,340 feet and a free-stream Mach number of 0.55. The rocket was ignited by delay squibs 5.7 seconds after release and the model accelerated to a maximum velocity of 5015 feet per second and a Mach number of 5.02 during the following 6.7 seconds. A peak acceleration of 1093 feet per second per second was observed just after rocket ignition. At peak Mach number, the model was at an altitude of 27,000 feet and the free-stream and cone Reynolds numbers were 15.9 and 23×10^6 per foot, respectively. The maximum local Reynolds number on the cone at a slant distance of 25.84 inches from the cone apex was 50×10^6. After rocket burn-out, the model decelerated because of drag, reaching a maximum deceleration of -365 feet per second per second at 13.4 seconds after release. The inflections in the deceleration curve between 27.5 and 33 seconds are due to changes in the aerodynamic drag forces as the

model passed through the transonic Mach number region. At 37 seconds after release, the model reached sea level and had decelerated to a Mach number of 0.90.

Time histories of skin temperatures t_s at seven locations are presented in figure 8. Also shown are the free-stream total temperature T_0, adiabatic wall temperature T_{aw}, static temperature just outside the cone boundary layer t_δ, and free-stream static temperature t_0.

Because of transient flight conditions, the missile skin is, except for an instant near peak skin temperatures, always being heated or cooled by the boundary layer. The rate at which the skin is being heated or cooled is a function of the total energy in the boundary layer and also of the state (laminar or turbulent) of the boundary layer. Since the total energy in the boundary layer changes smoothly with time, any abrupt change in the time rate of change of the skin temperature can only indicate corresponding changes in the boundary-layer heat-transfer coefficient. The heat-transfer coefficient h is shown in figure 9 for a typical temperature element. The boundary-layer heat-transfer coefficient is directly related to the state of the boundary layer so that while the skin is being heated, a sudden increase in the slope of the skin-temperature curve indicates boundary-layer transition from laminar to turbulent flow. An abrupt decrease in the slope of the skin-temperature curve indicates boundary-layer transition from turbulent to laminar flow. In figure 8, for each of the temperature elements, two distinct changes in slope are apparent between 9.3 and 11.2 seconds. The first is a decrease in slope and the second an increase in slope, indicating transition from turbulent to laminar flow and then from laminar to turbulent flow.

The ratio of skin temperature to local static temperature just outside the boundary layer t_s/t_δ is plotted against local Mach number on the cone M_δ for the various stations in figure 10. The two transition points for each station are indicated on the curves and the local Reynolds number for each is given. Van Driest has shown (ref. 2) that the required temperature ratio for boundary-layer stability at Mach numbers greater than 2.0 is essentially the same for all Reynolds numbers from 8×10^4 to infinity. Consequently, the analytical solution of the boundary-layer stability equation based on infinite Reynolds number is equal to the solution at the finite Reynolds numbers encountered in this investigation. The theoretical curve from reference 2 is presented in figure 10 and compared with the experimental data.

As the model penetrates the infinite stability region during acceleration, the boundary layer is observed to go from turbulent to laminar for each of the stations. However, at local Mach numbers from about 3.5

to 4.0, and at wall to local stream temperature ratios of about 1.2 to 1.3, the flow is observed to go back to turbulent. These values of t_s/t_δ and local Mach number are well within the theoretically stable region. The local Reynolds number at which these transitions occurred varied from 9×10^6 to 32×10^6 based on slant distance from the cone apex. The transition was observed under nearly identical conditions at the two 23.53-inch stations, which were 180° apart.

The temperature ratio at which transition occurred is plotted against local Reynolds number at the instant of transition for the various stations in figure 11. The data are plotted separately for the turbulent-to-laminar and laminar-to-turbulent cases. Local Mach numbers for each point are indicated on the curves. Also shown is one of Van Driest's solutions (for Prandtl number of 0.75 and Sutherland viscosity law) for temperature ratio required for infinite stability at Mach numbers of 2.5, 3.0, and 4.0 on a flat plate. The local Mach number at which transition occurred varied from 2.67 to 2.74 in figure 11(a) and from 3.45 to 3.93 in figure 11(b). It is apparent from the shape of the experimental curve that further small decreases in temperature ratio might lead to appreciably higher transition Reynolds numbers. It is of interest that in reference 4, there is an indication of a transition from turbulent to laminar flow on a 20° cone at a Reynolds number of 90×10^6, local stream Mach number of 2.3, and skin to local stream temperature ratio of about 1.20.

In figure 12, the data of figure 11 are combined and compared with recent tunnel results of a boundary-layer stability investigation conducted on a 10° cone (ref. 8) at a free-stream Mach number of 3.12 (cone Mach number of 3.02). The maximum transition Reynolds number of the tunnel tests was about 10.6×10^6. The tunnel model had a surface finish of the order of 16 micro inch rms (somewhat rougher than that of the flight model). The results of the tunnel and flight investigations appear to agree within the scatter of the data at a Reynolds number of about 10×10^6. The tunnel and flight cone Mach numbers at this condition were 3.02 and 2.7, respectively.

The significance of the agreement between the wind-tunnel and flight data at a Reynolds number of 10×10^6 is difficult to assess with the limited amount of data at hand. The agreement may indicate that at these conditions there is no appreciable effect of using a surface finish finer than the tunnel value of about 16 rms and that the turbulence level that existed in the tunnel (0.5 to 1.0 percent) did not affect results at a Reynolds number of 10×10^6. Apparently the flight data provide an excellent extension of the tunnel data to high Reynolds numbers.

The flight data at Reynolds numbers near 20×10^6 indicate little Mach number effect on stability criteria at local stream Mach numbers between 2.68 and 3.92.

A large amount of data is believed to be required before actual boundary-layer stability criteria can be determined. However, from the limited data of the flight, it appears that with a 20° cone polished to a surface finish of 1.5 to 2.0 micro inch rms and flown under actual atmospheric conditions, the temperature ratio required for boundary-layer stabilization at high Reynolds numbers is lower than that predicted by Van Driest when his solution is based on a Prandtl number of 0.75 and the Sutherland viscosity law.

A Prandtl number of 0.75 and the Sutherland viscosity law are believed to be reasonable assumptions for calculating the boundary-layer stability criteria for the range of conditions encountered during this investigation. However, in reference 2, calculations are also based on the assumption of viscosity proportional to temperature and a Prandtl number of 1.0. Shown in figure 13 is a comparison of the conditions at which transition was observed in flight with Van Driest's infinite-stability-criteria solutions for the various assumptions. Although boundary-layer stability or instability and boundary-layer transition are not synonymous, the conditions under which transition occurs in this investigation are probably indicative of boundary-layer stability criteria. If this is assumed to be true, the observed transition conditions for the configuration flown indicate that the Van Driest solution based on a Prandtl number of 1.0 and viscosity proportional to temperature gives a better prediction of stability criteria in the range of Mach numbers from 2.5 to 4.0.

A recent analysis by Dunn and Lin (ref. 9) considers the effects of three-dimensional disturbances on stability. Their solutions for three-dimensional disturbance stability criteria at a local Mach number of 4.0 and based on a Prandtl number of 0.75 indicate a lower temperature ratio required for stability than does Van Driest's analysis for the two-dimensional disturbance with the same Prandtl number and viscosity relation. The solution at Mach 4.0 shown in figure 13 is in closer agreement with the experimental data shown than is the stability criteria based on two-dimensional disturbances. Complete solutions for the three-dimensional case have not as yet been made, so that comparisons at other Mach numbers are not available.

At appreciably higher free-stream Mach numbers than covered here but with the same range of local cone Mach numbers, the high air temperature in the conical flow field and in the boundary layer will have an appreciable effect on Prandtl number and viscosity. Caution should therefore be used in applying results of the present investigation to high free-stream Mach numbers with blunt cones, even though the local Mach number, Reynolds number, and temperature ratios may be comparable in both cases.

CONCLUSIONS

A highly polished 20° included-angle cone-cylinder body of revolution has been flown to obtain boundary-layer transition data at low ratios of wall to local stream temperature. The following results have been obtained:

1. A maximum free-stream Mach number of 5.02 and maximum local Reynolds number on the cone of 50×10^6 were reached during the flight.

2. Transition from a turbulent to a laminar and from a laminar to a turbulent boundary layer were observed at each of seven measuring stations on the cone. The minimum and maximum transition Reynolds numbers observed were 9×10^6 and 32×10^6, respectively. The maximum transition Reynolds number occurred at a local Mach number of 3.56 with a wall to local stream temperature ratio of 1.20.

3. If it is assumed that conditions under which boundary-layer transition occur in this investigation are indicative of boundary-layer stability criteria, the data suggest:

   a. Van Driest's solutions for the stability criteria based on two-dimensional disturbances and a Prandtl number of 1.00 with viscosity proportional to temperature closely approximate the free-flight data at local Mach numbers from 2.5 to 4.0 and at Reynolds numbers from 9×10^6 to 32×10^6.

   b. The experimental temperature ratio for boundary-layer stability at a local Mach number of 4.0 is closer to the value calculated by Dunn and Lin than that calculated by Van Driest. The analyses by Dunn and Lin and Van Driest are for similar assumptions (Prandtl number of 0.75, infinite Reynolds number, and linear viscosity-temperature relation) but differ in the type of boundary-layer disturbance. Dunn and Lin assume three-dimensional disturbances, whereas Van Driest assumes two-dimensional disturbances. The three-dimensional analysis gives a temperature ratio of 1.47 as compared with 1.65 for the two-dimensional analysis and approximately 1.30 for the experimental data at a local Mach number of 4.0.

Lewis Flight Propulsion Laboratory
National Advisory Committee for Aeronautics
Cleveland, Ohio, September 15, 1955

REFERENCES

1. Lees, Lester: The Stability of the Laminar Boundary Layer in a Compressible Fluid. NACA Rep. 876, 1947. (Supersedes NACA TN 1360.)

2. Van Driest, E. R.: Calculation of the Stability of the Laminar Boundary Layer in a Compressible Fluid on a Flat Plate with Heat Transfer. Jour. Aero. Sci., vol. 19, no. 12, Dec. 1952, pp. 801-812.

3. Czarnecki, K. R., and Sinclair, Archibald R.: Factors Affecting Transition at Supersonic Speeds. NACA RM L53I18a, 1953.

4. Sternberg, Joseph: A Free-Flight Investigation of the Possibility of High Reynolds Number Supersonic Laminar Boundary Layers. Jour. Aero. Sci., vol. 19, no. 11, Nov. 1952, pp. 721-723.

5. Messing, Wesley E., Rabb, Leonard, and Disher, John H.: Preliminary Drag and Heat-Transfer Data Obtained from Air-Launched Cone-Cylinder Test Vehicle over Mach Number Range from 1.5 to 5.18. NACA RM E53I04, 1953.

6. Rabb, Leonard, and Simpkinson, Scott H.: Free-Flight Heat-Transfer Measurements on Two 20°-Cone-Cylinders at Mach Numbers from 1.3 to 4.9. NACA RM E55F27, 1955.

7. Fricke, Clifford L., and Smith, Francis B.: Skin-Temperature Telemeter for Determining Boundary-Layer Heat-Transfer Coefficients. NACA RM L50J17, 1951.

8. Jack, John R., and Diaconis, N. S.: Variation of Boundary-Layer Transition with Heat Transfer on Two Bodies of Revolution at a Mach Number of 3.12. NACA TN 3562, 1955.

9. Dunn, D. W., and Lin, C. C.: On the Stability of the Laminar Boundary Layer in a Compressible Fluid. Jour. Aero. Sci., vol. 22, no. 7, July 1955, pp. 455-477.

Model Specifications	
Gross weight at launching, lb	197.6
Weight at end of rocket boost, lb	93
Launching altitude, ft	35,340
Center of gravity at launching (station), in.	49.9
Center of gravity at end of rocket boost (station), in.	47.2
Cross-sectional area (max.), sq ft	0.466
Skin thickness at temperature measuring stations, in.	0.0295 to 0.0321
Skin thickness of shell, in.	0.032
Fin area (2 fins), sq in.	152
Stabilizing-fin root-chord - thickness ratio	0.011

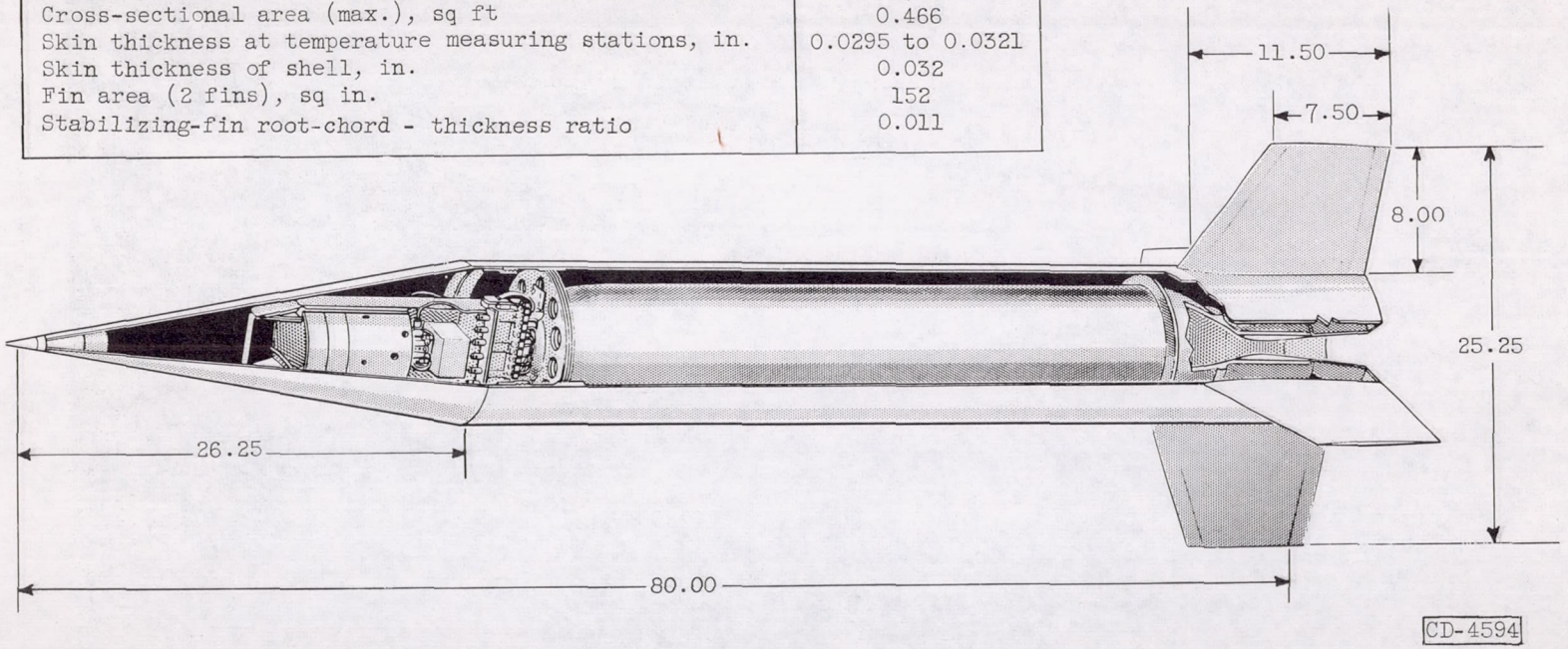

Figuare 1. - Dimensions and specifications of model.

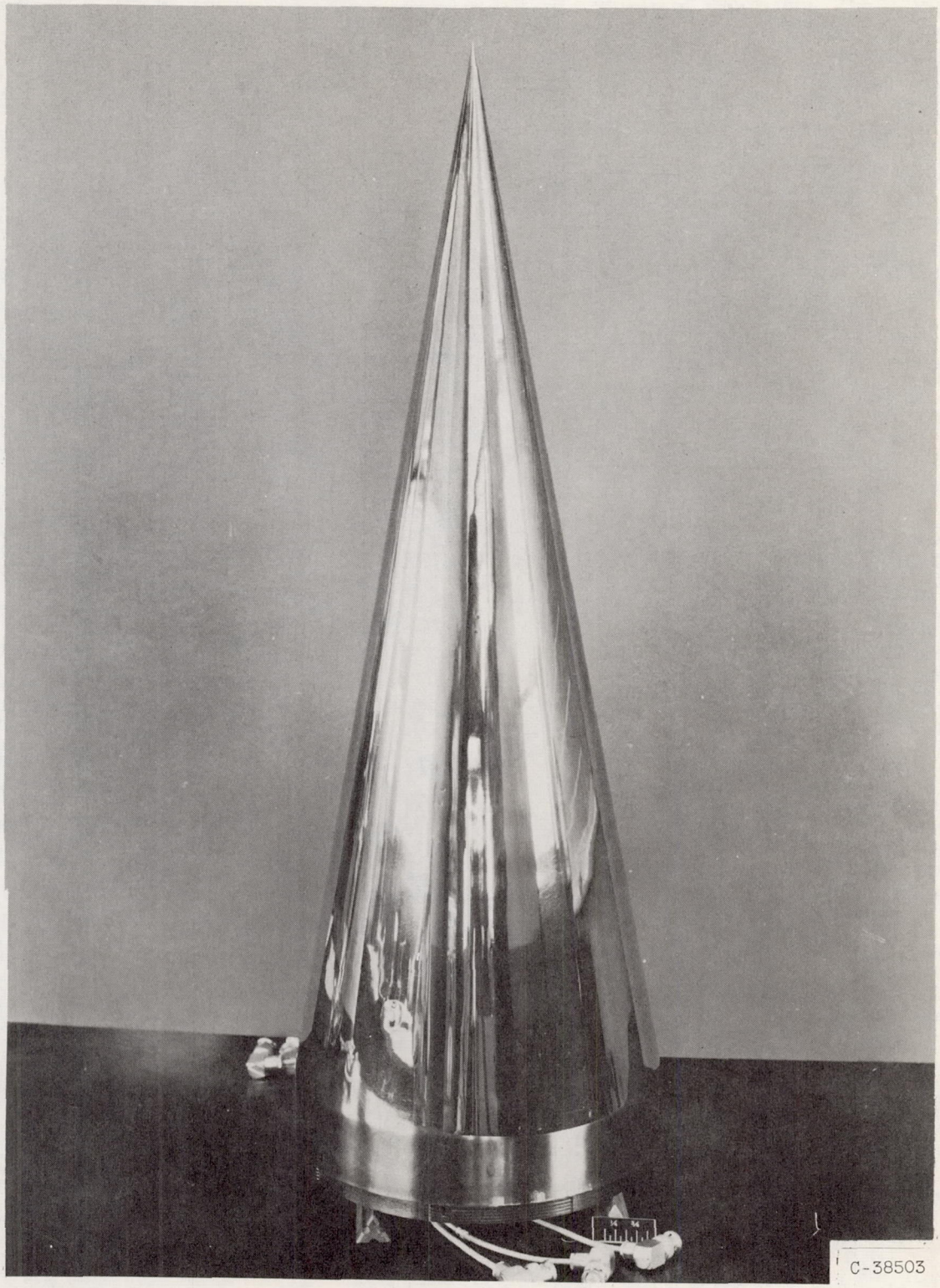

Figure 2. - Instrumented cone.

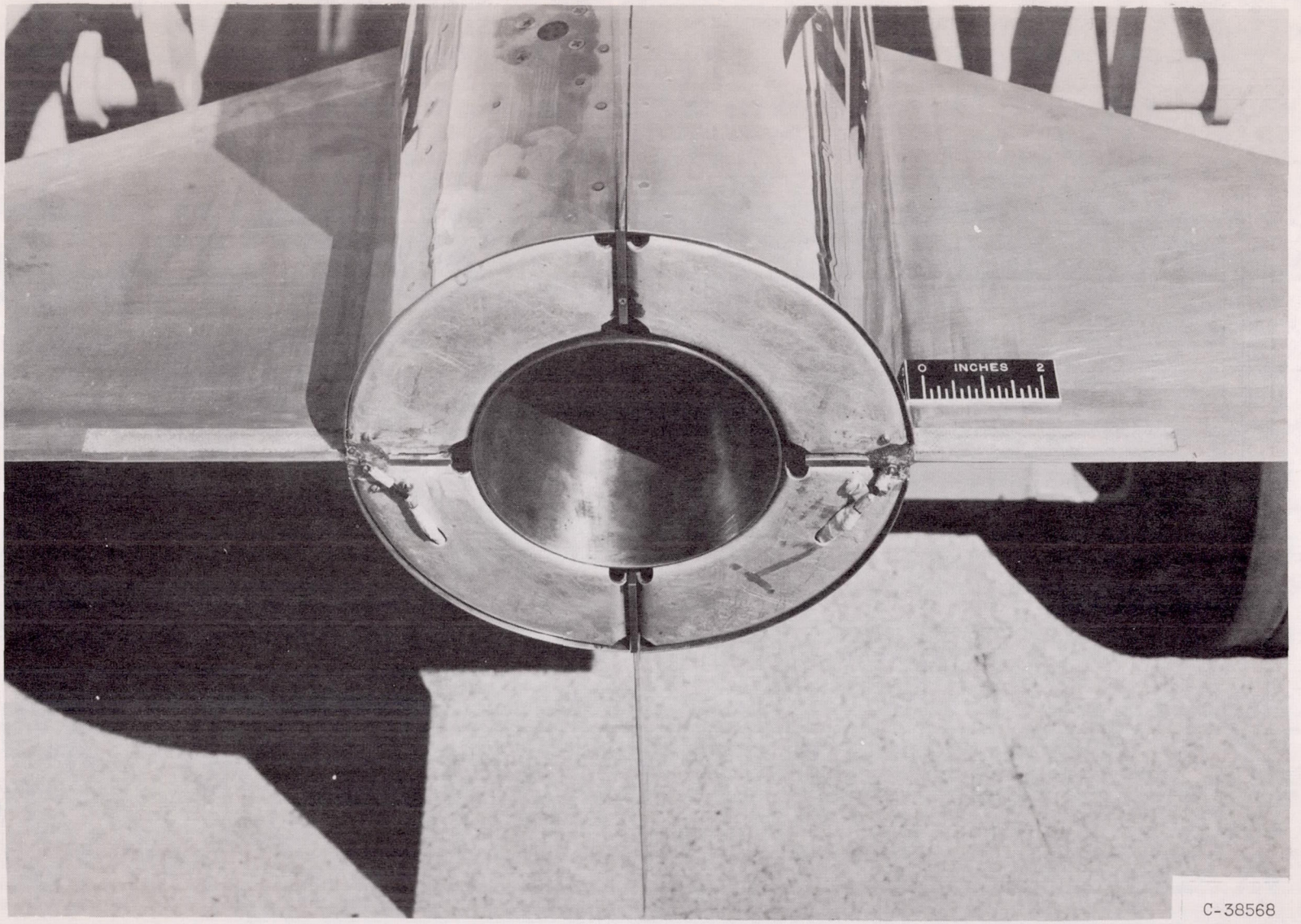

Figure 3. - Photograph of fins showing telemeter antenna installation.

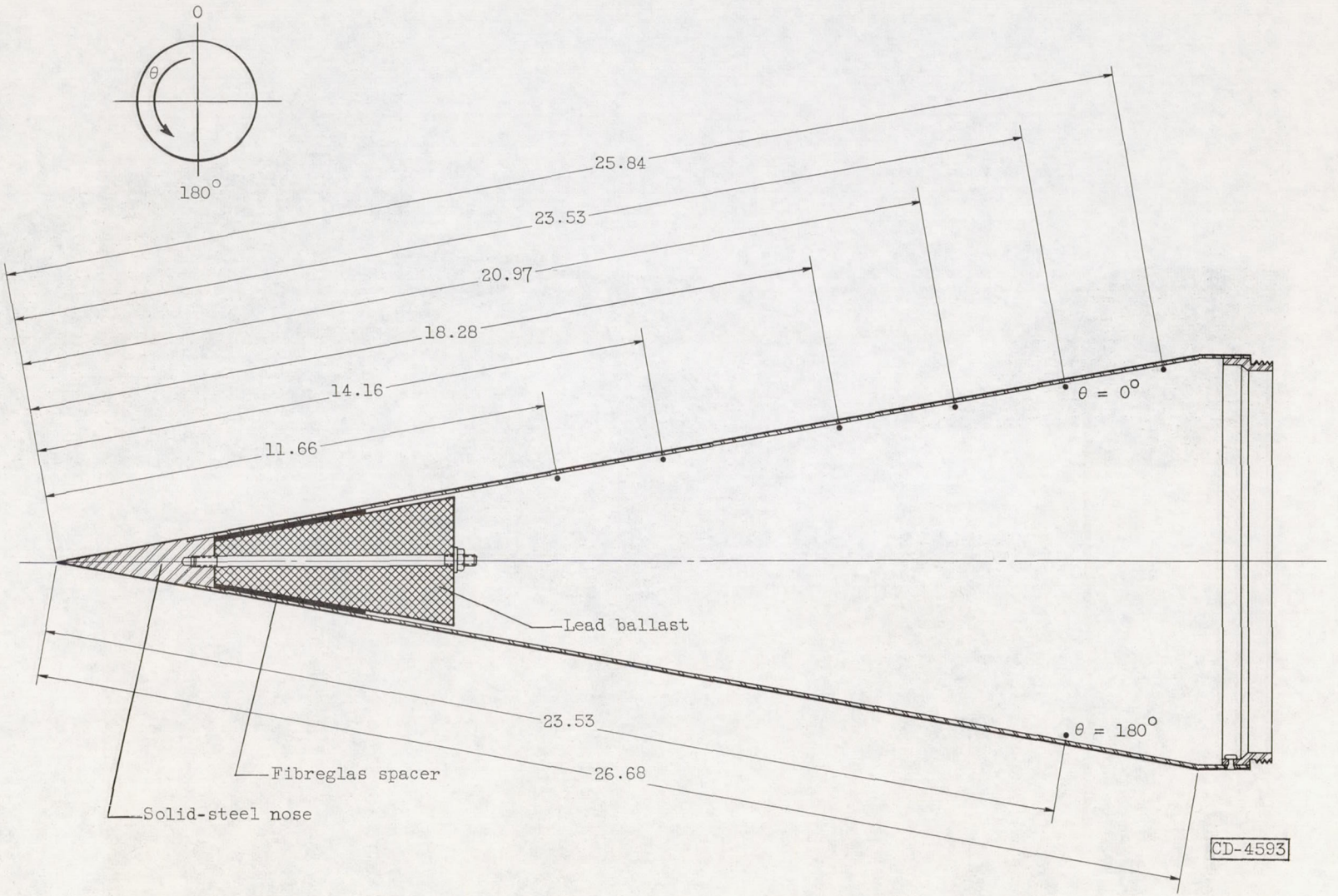

Figure 4. - Sketch of cone showing temperature-element locations. (All dimensions in inches.)

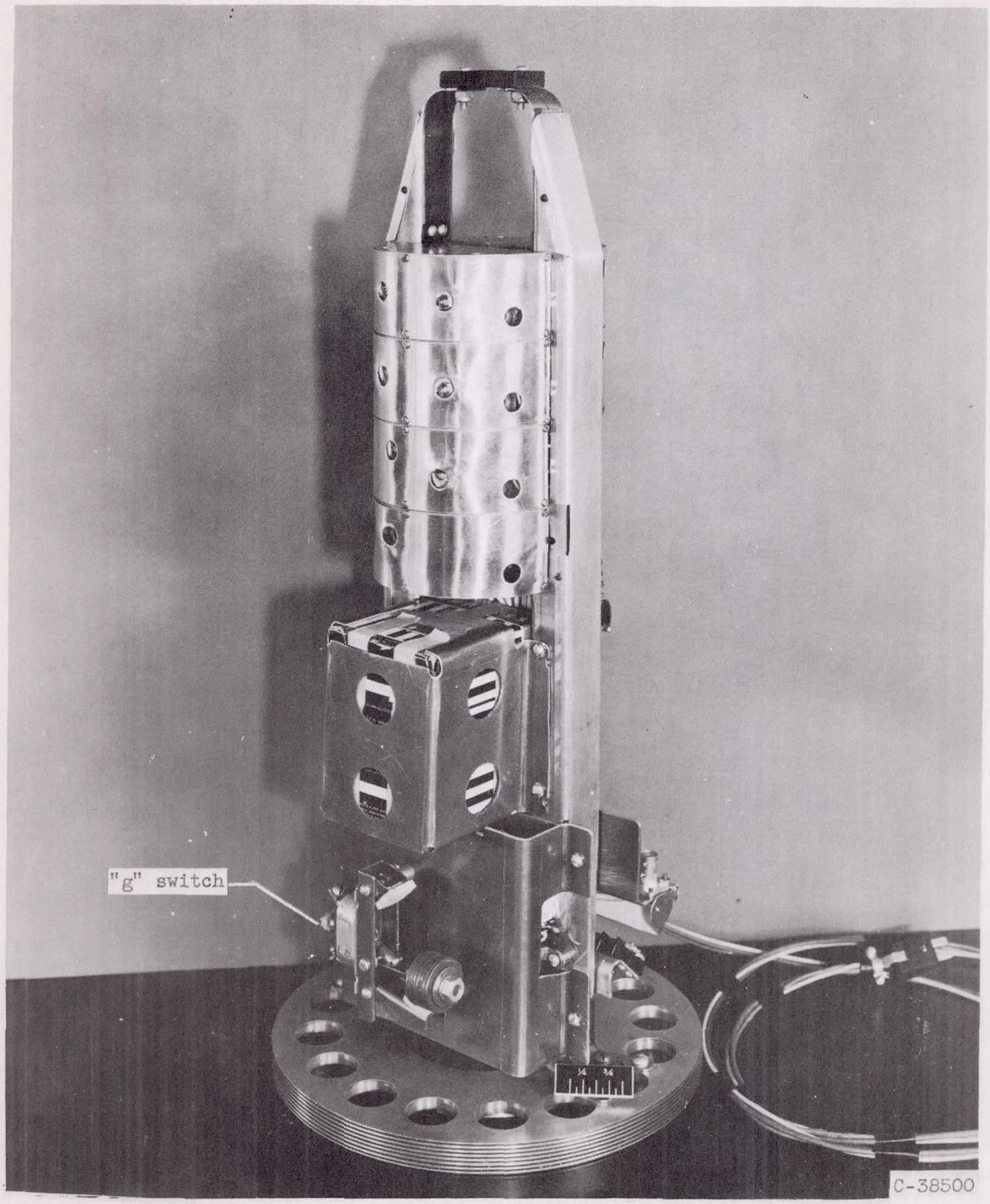

Figure 5. - Photograph of telemeter assembly showing "g" switch.

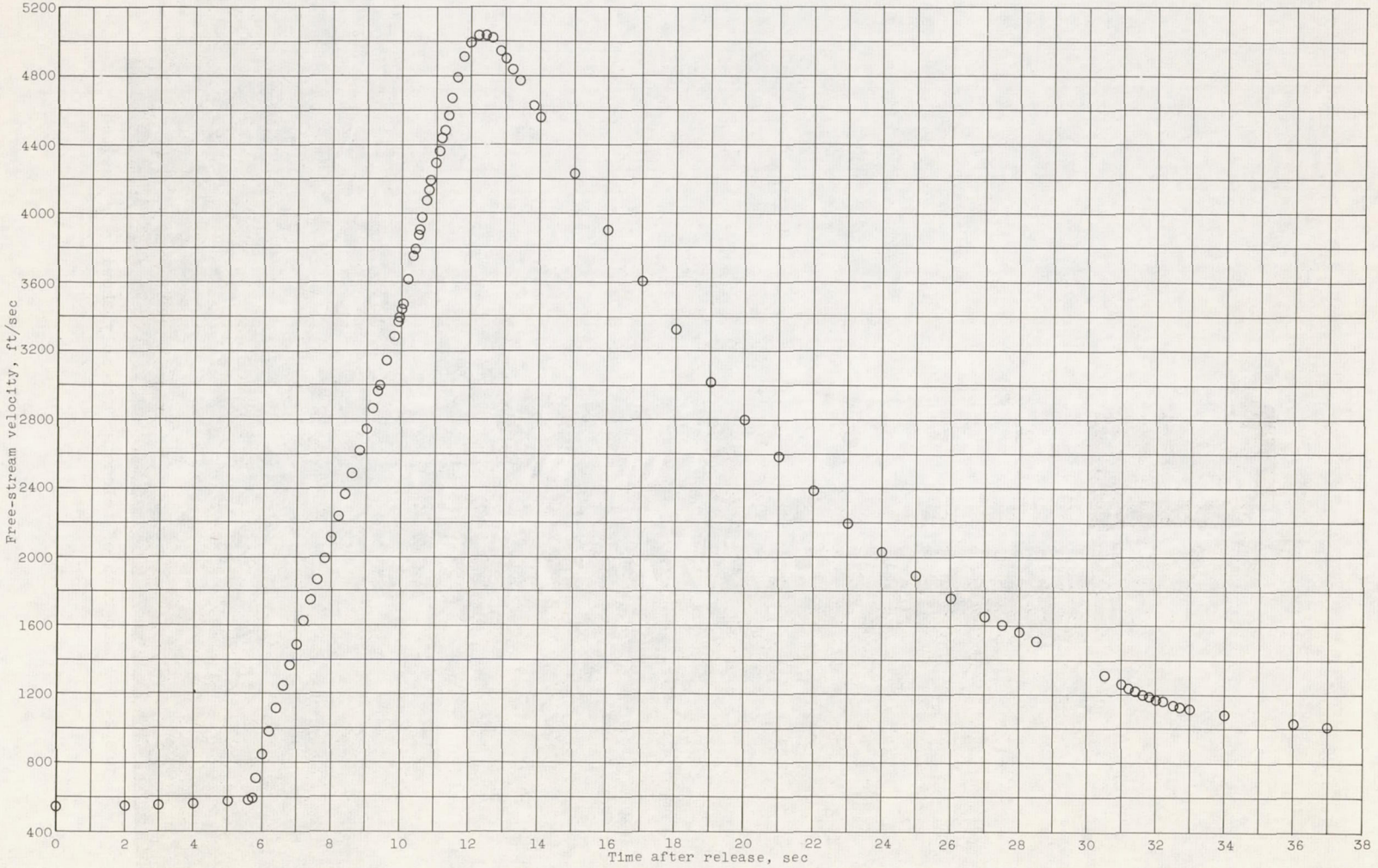

(a) Free-stream velocity.

Figure 6. - Variation of flight conditions with time.

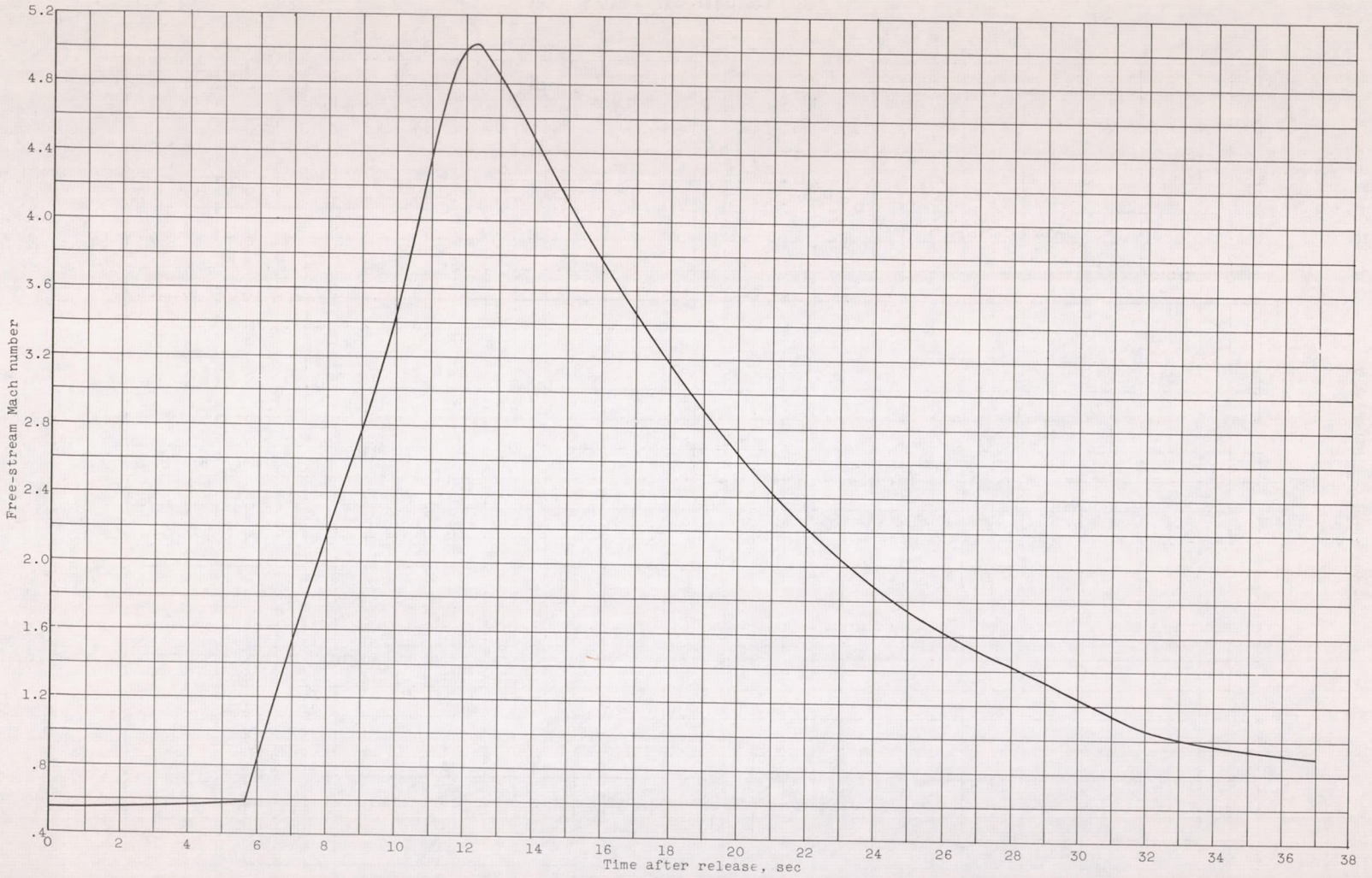

(b) Free-stream Mach number.

Figure 6. - Continued. Variation of flight conditions with time.

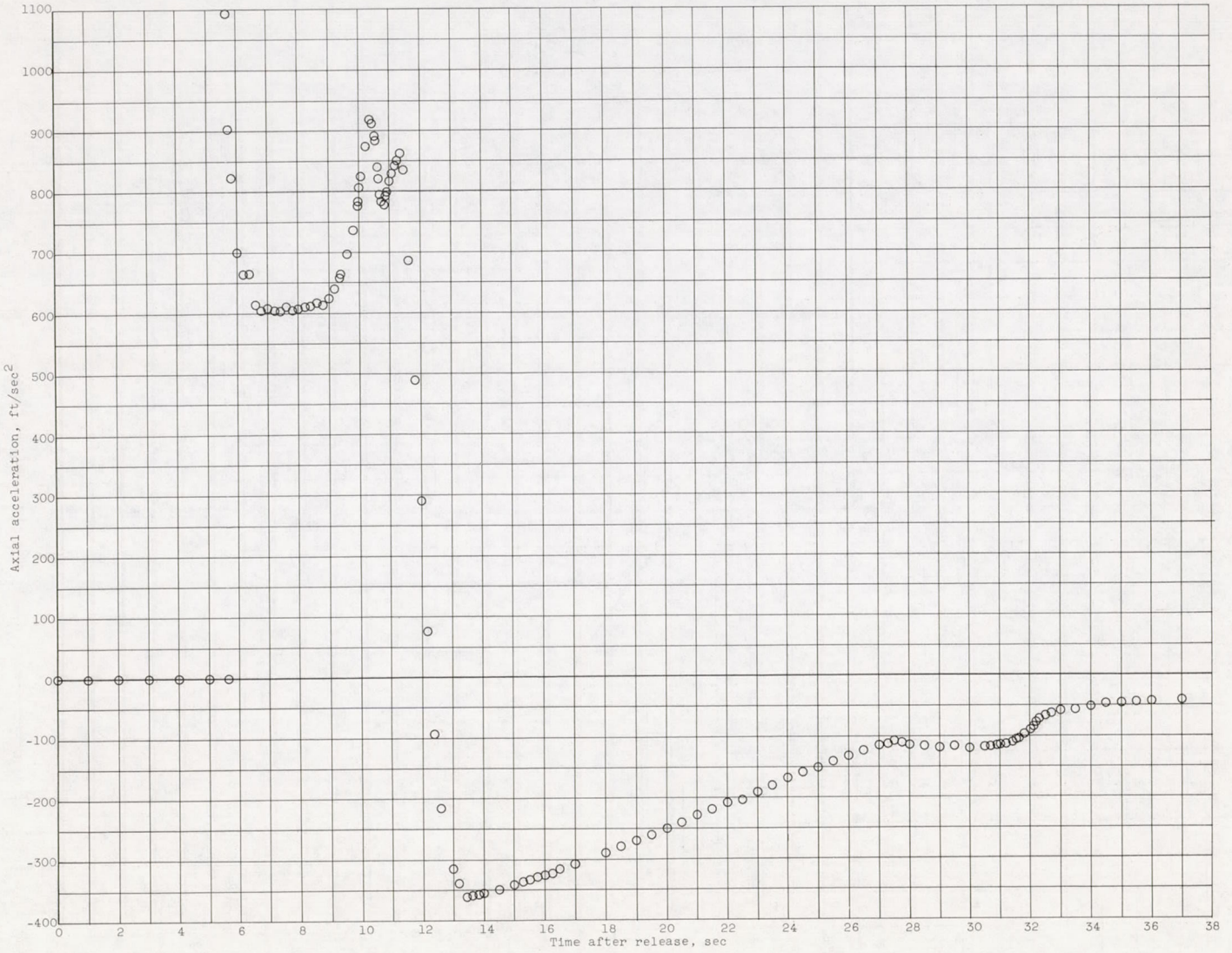

(c) Axial acceleration.

Figure 6. - Continued. Variation of flight conditions with time.

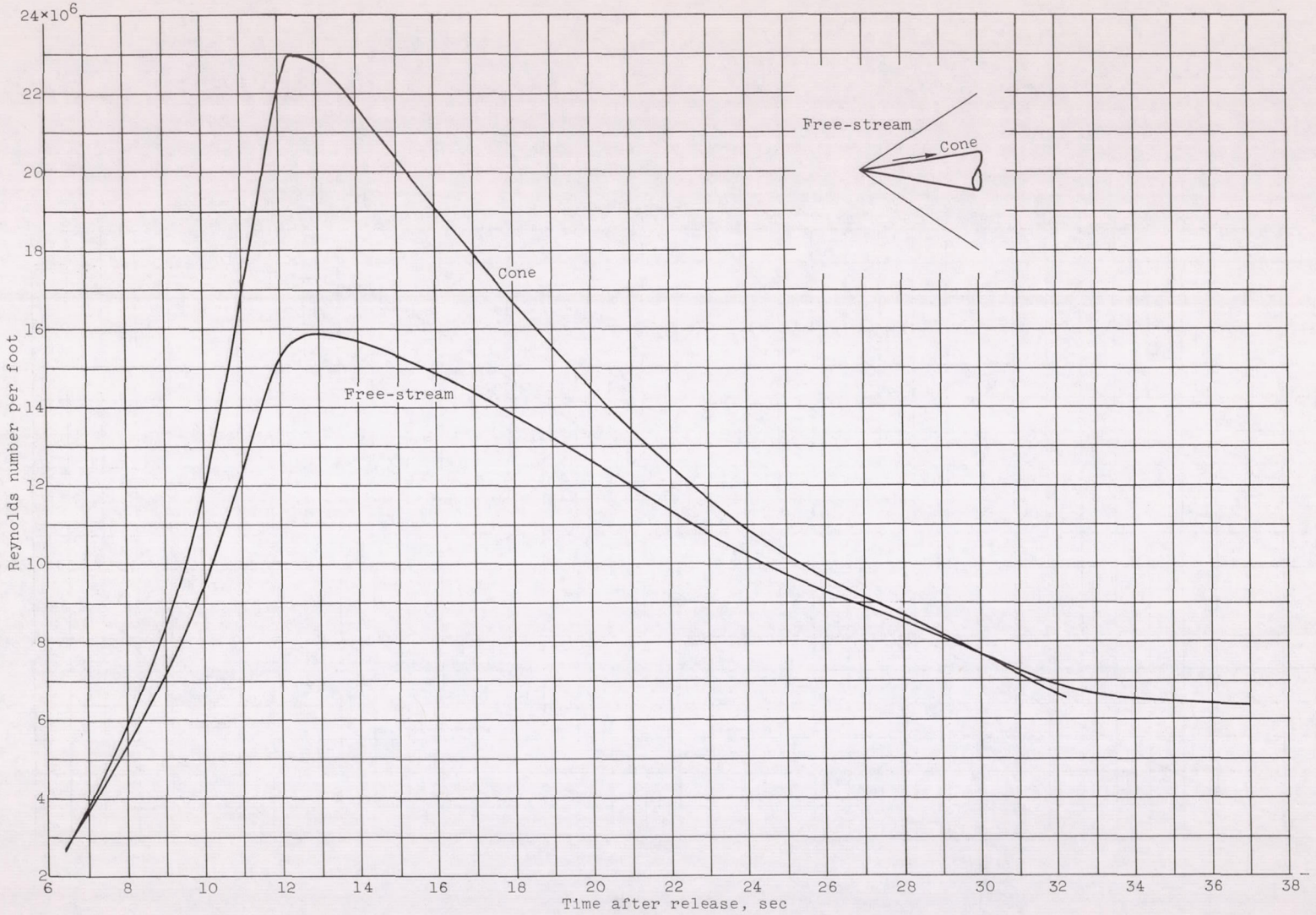

(d) Free-stream and cone Reynolds number per foot.

Figure 6. - Continued. Variation of flight conditions with time.

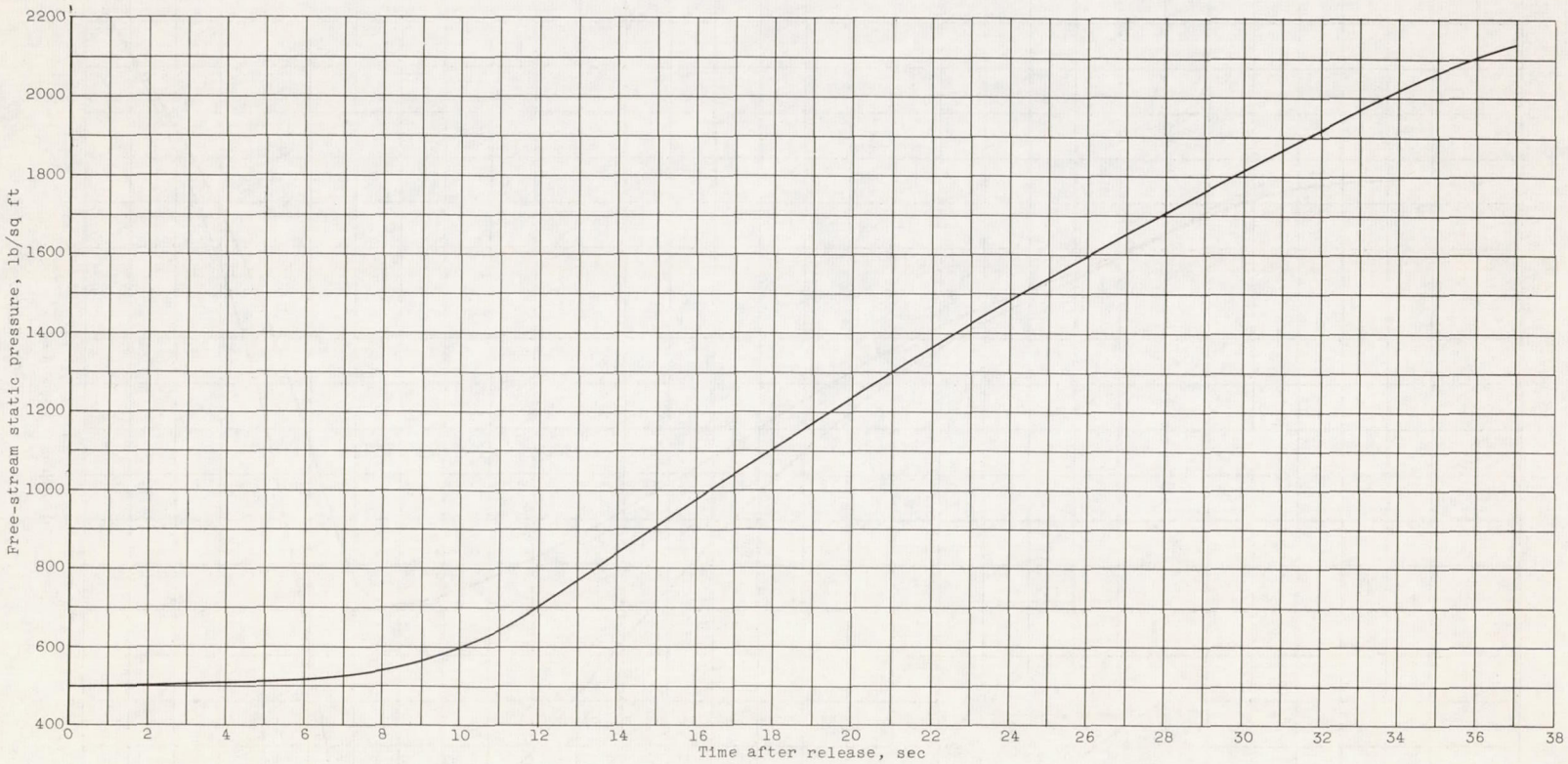

(e) Free-stream static pressure.

Figure 6. - Concluded. Variation of flight conditions with time.

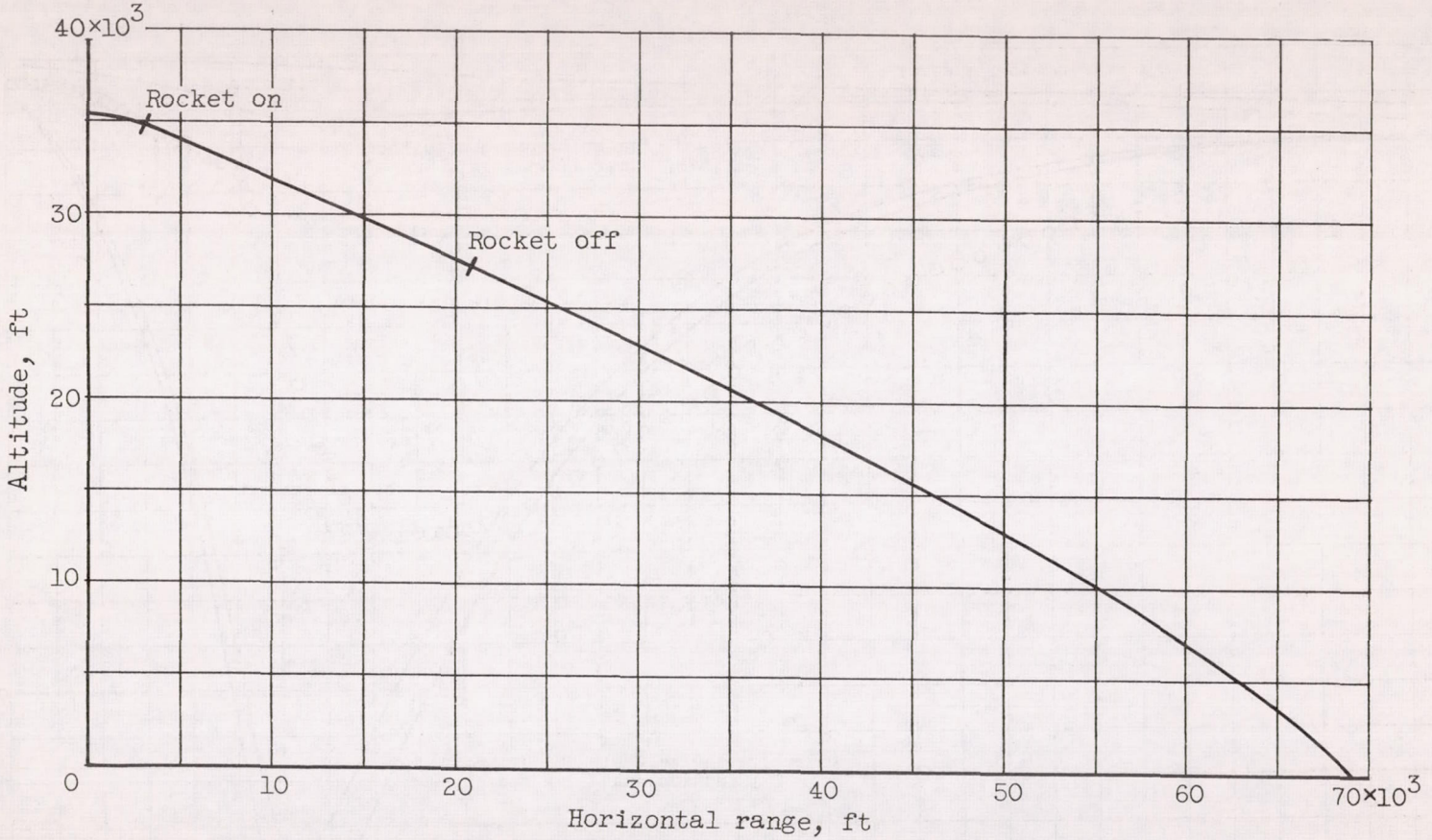

Figure 7. - Trajectory of 20-degree cone-cylinder test vehicle.

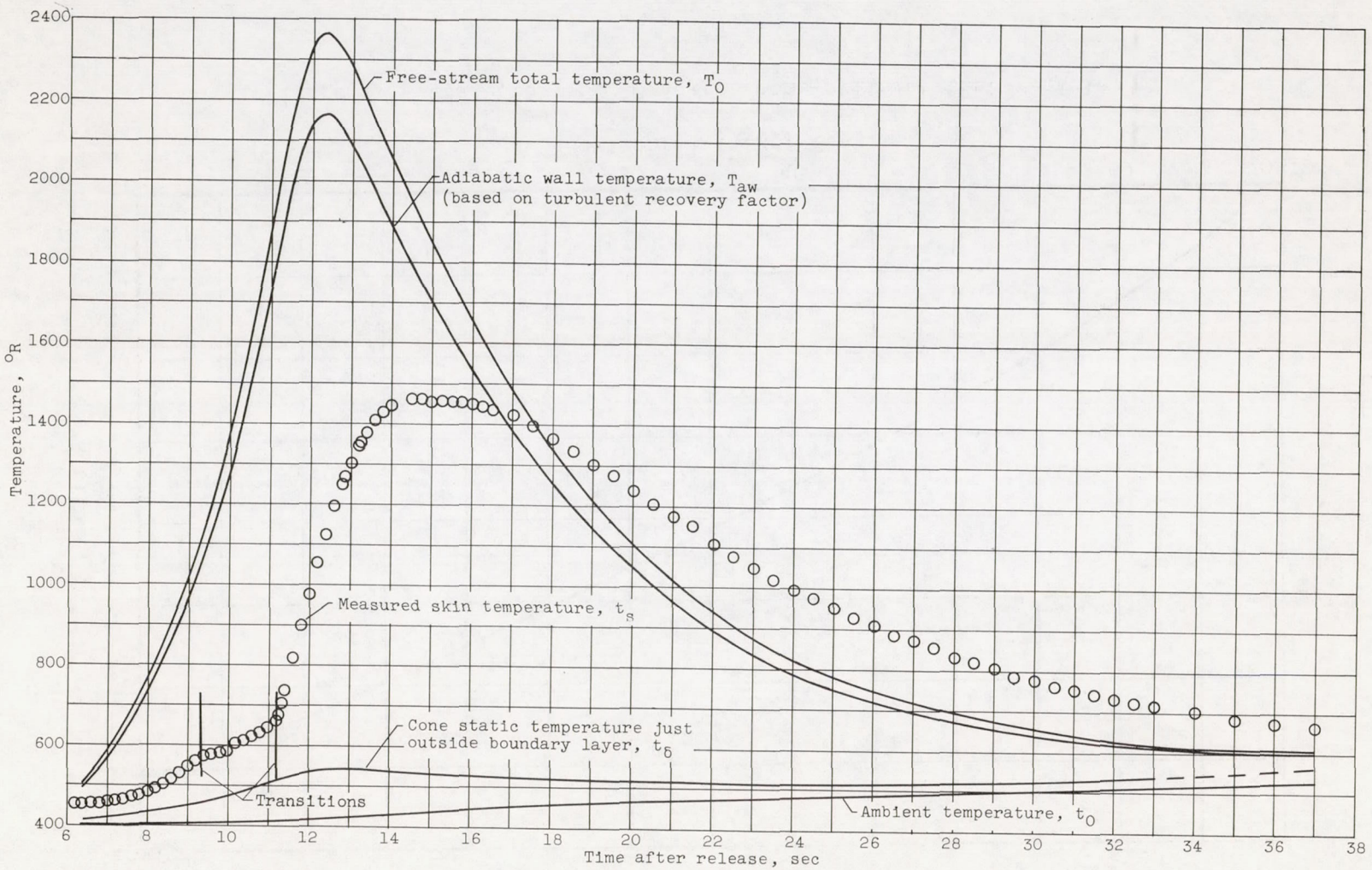

(a) Slant distance from cone apex, 11.66 inches.

Figure 8. - Time history of air and skin temperatures for 20-degree cone-cylinder test vehicle.

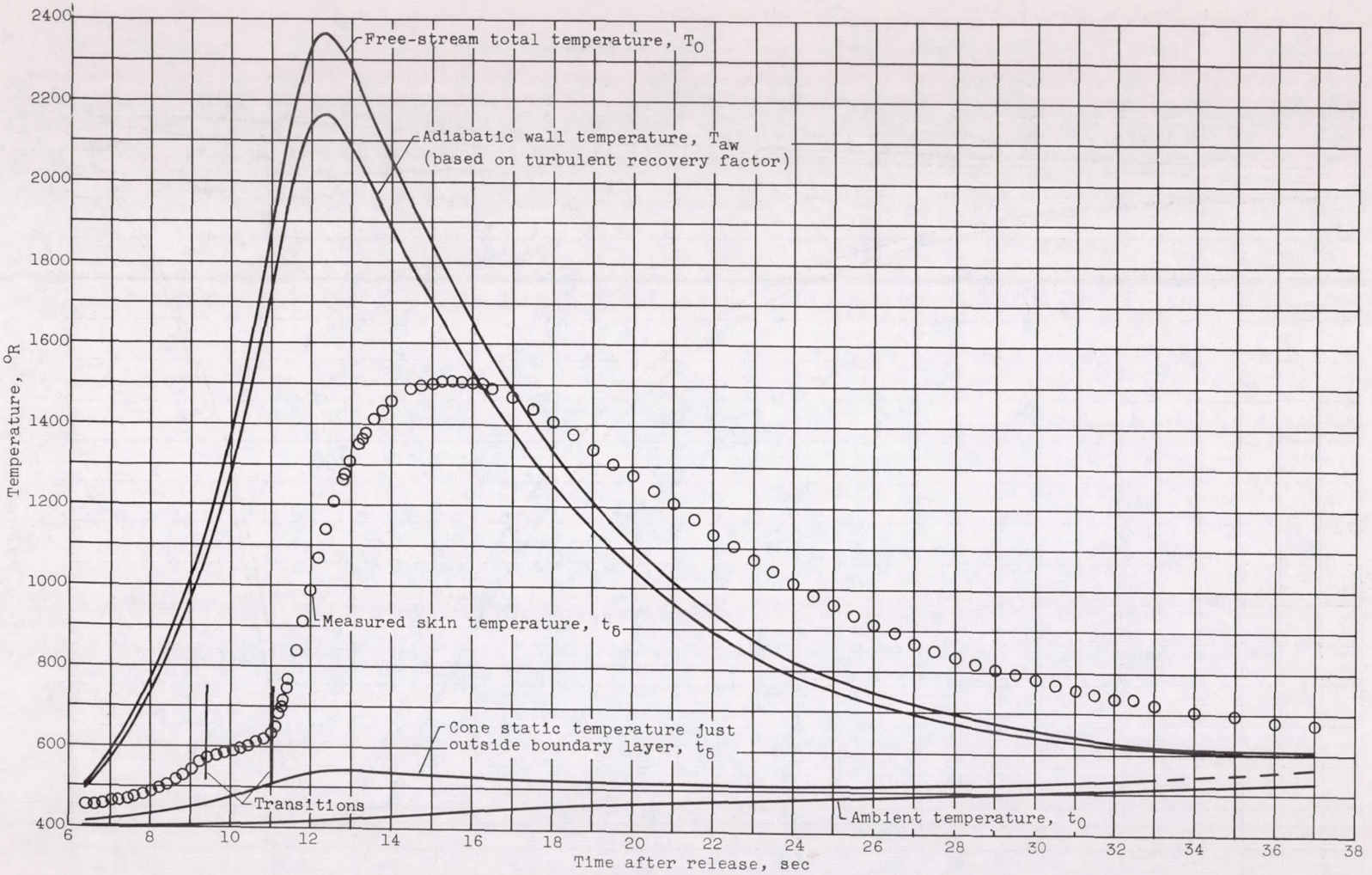

(b) Slant distance from cone apex, 14.16 inches.

Figure 8. - Continued. Time history of air and skin temperatures for 20-degree cone-cylinder test vehicle.

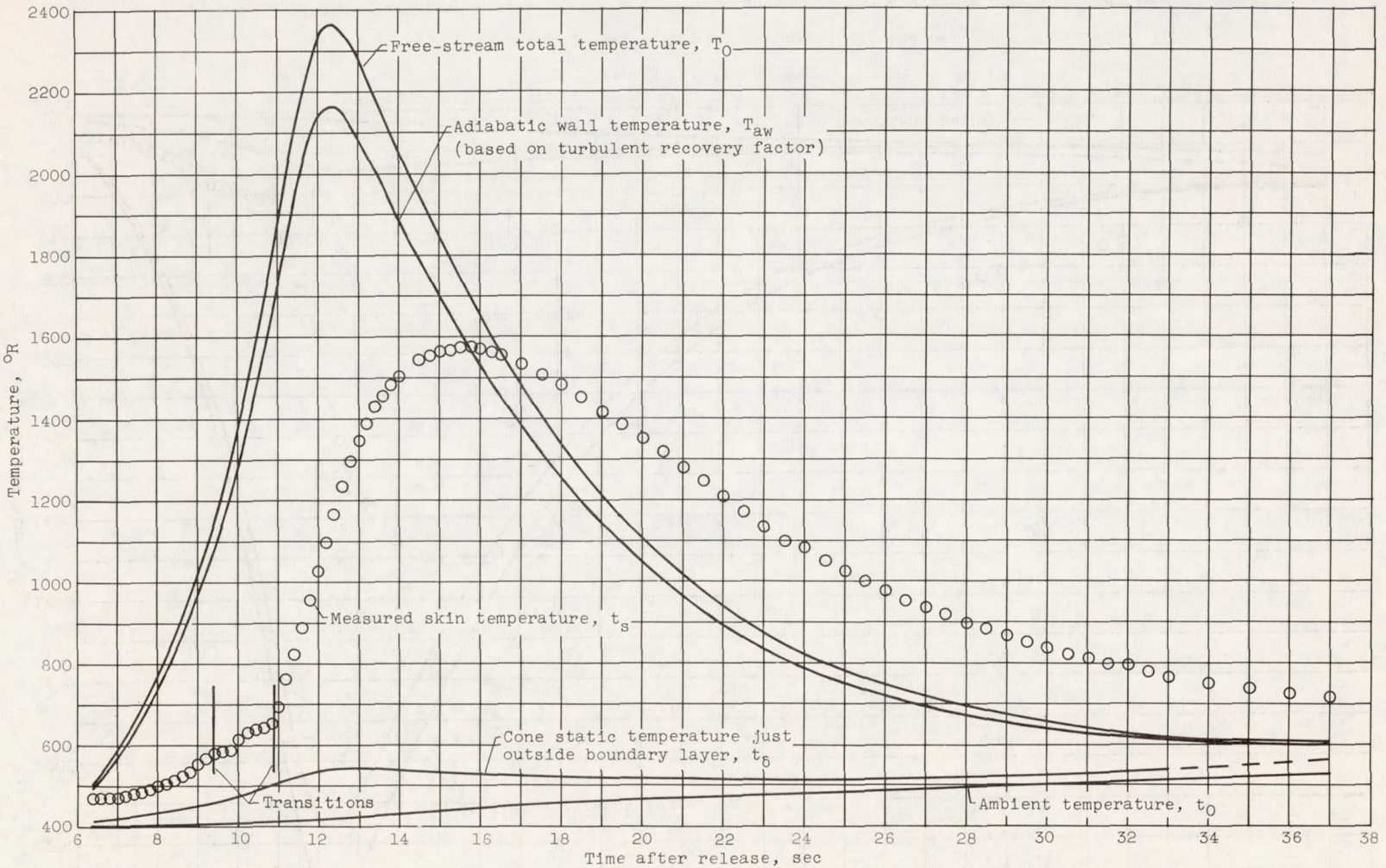

(c) Slant distance from cone apex, 18.28 inches.

Figure 8. - Continued. Time history of air and skin temperatures for 20-degree cone-cylinder test vehicle.

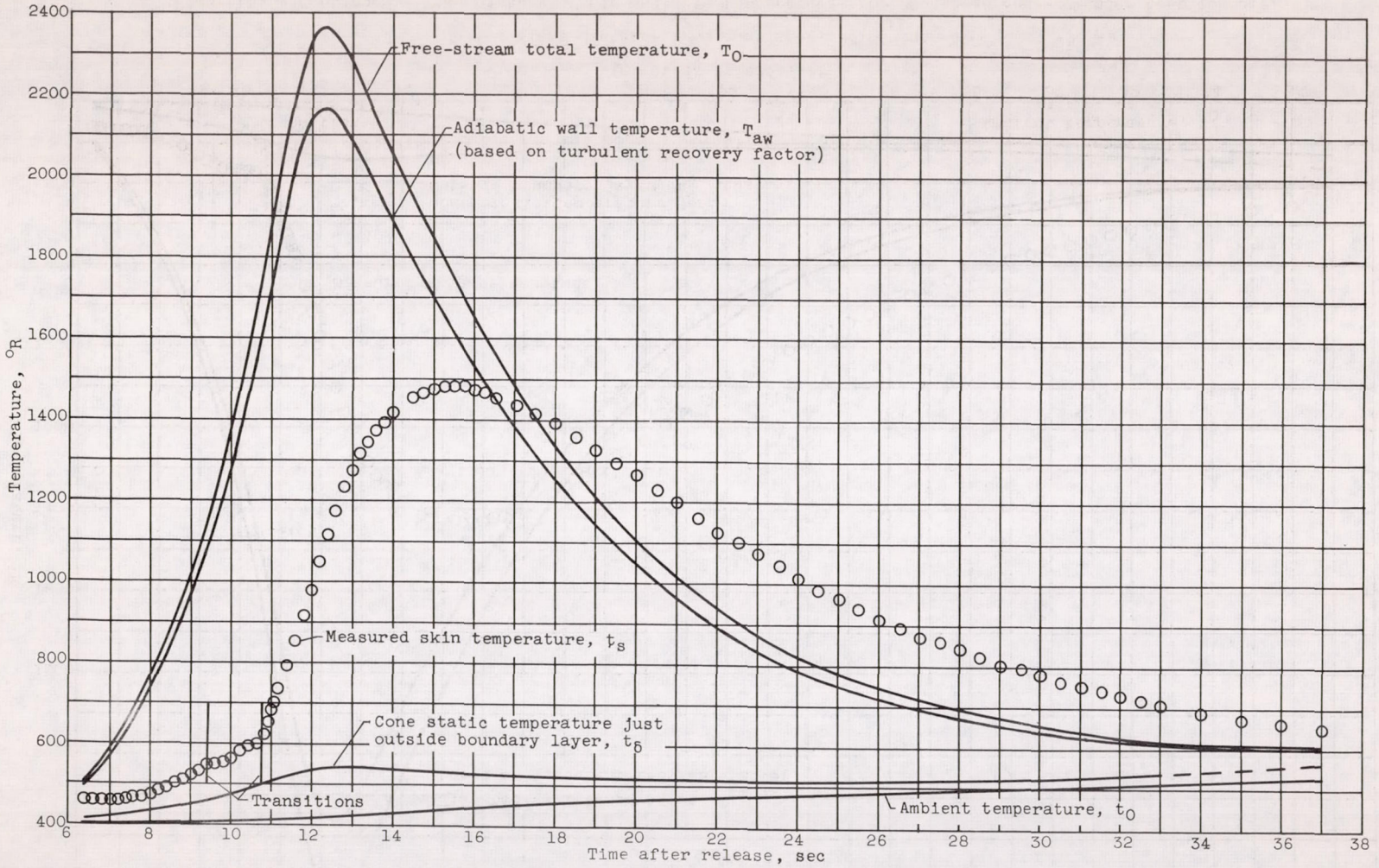

(d) Slant distance from cone apex, 20.97 inches.

Figure 8. - Continued. Time history of air and skin temperatures for 20-degree cone-cylinder test vehicle.

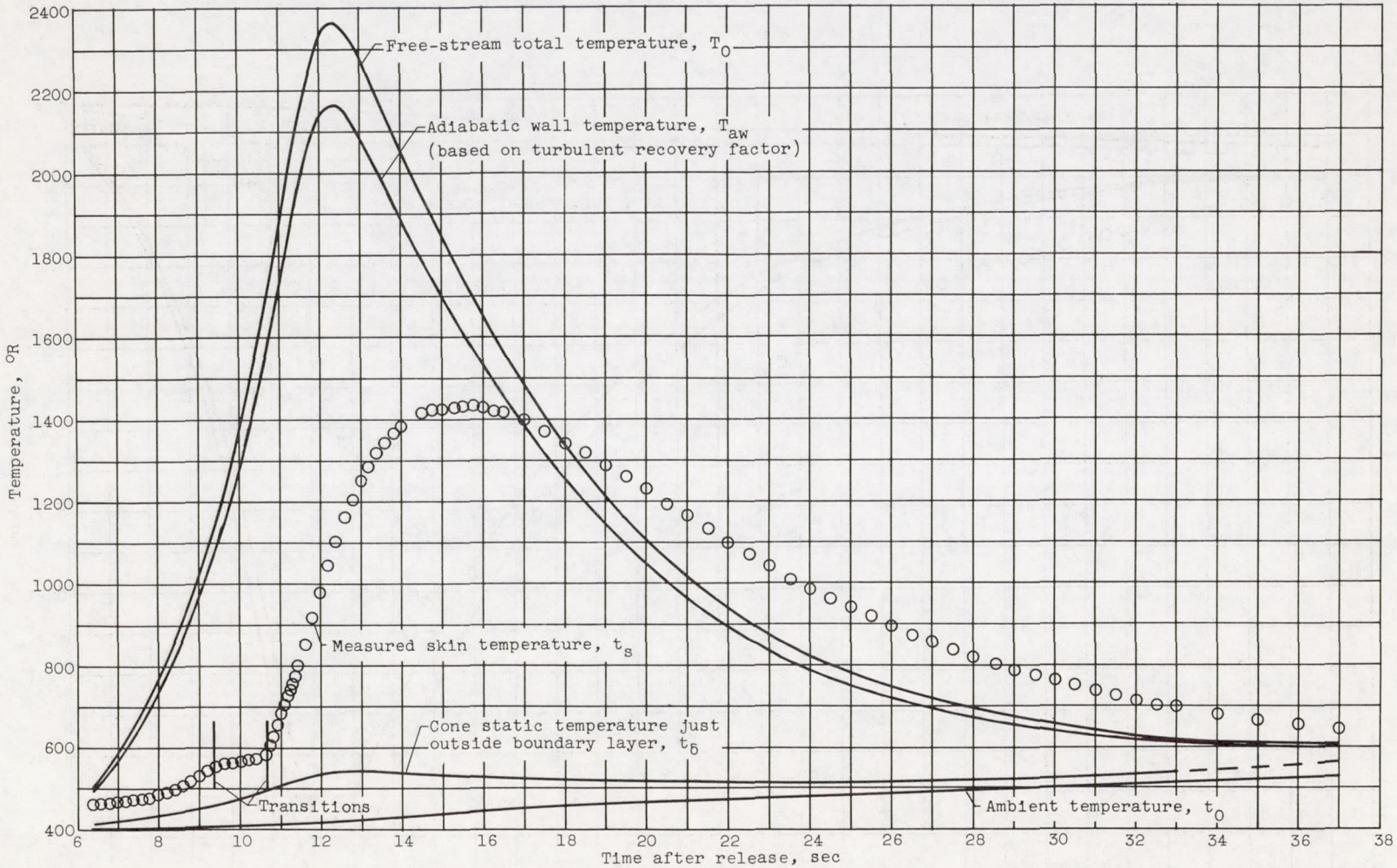

(e) Slant distance from cone apex, 23.53 inches.

Figure 8. - Continued. Time history of air and skin temperatures for 20-degree cone-cylinder test vehicle.

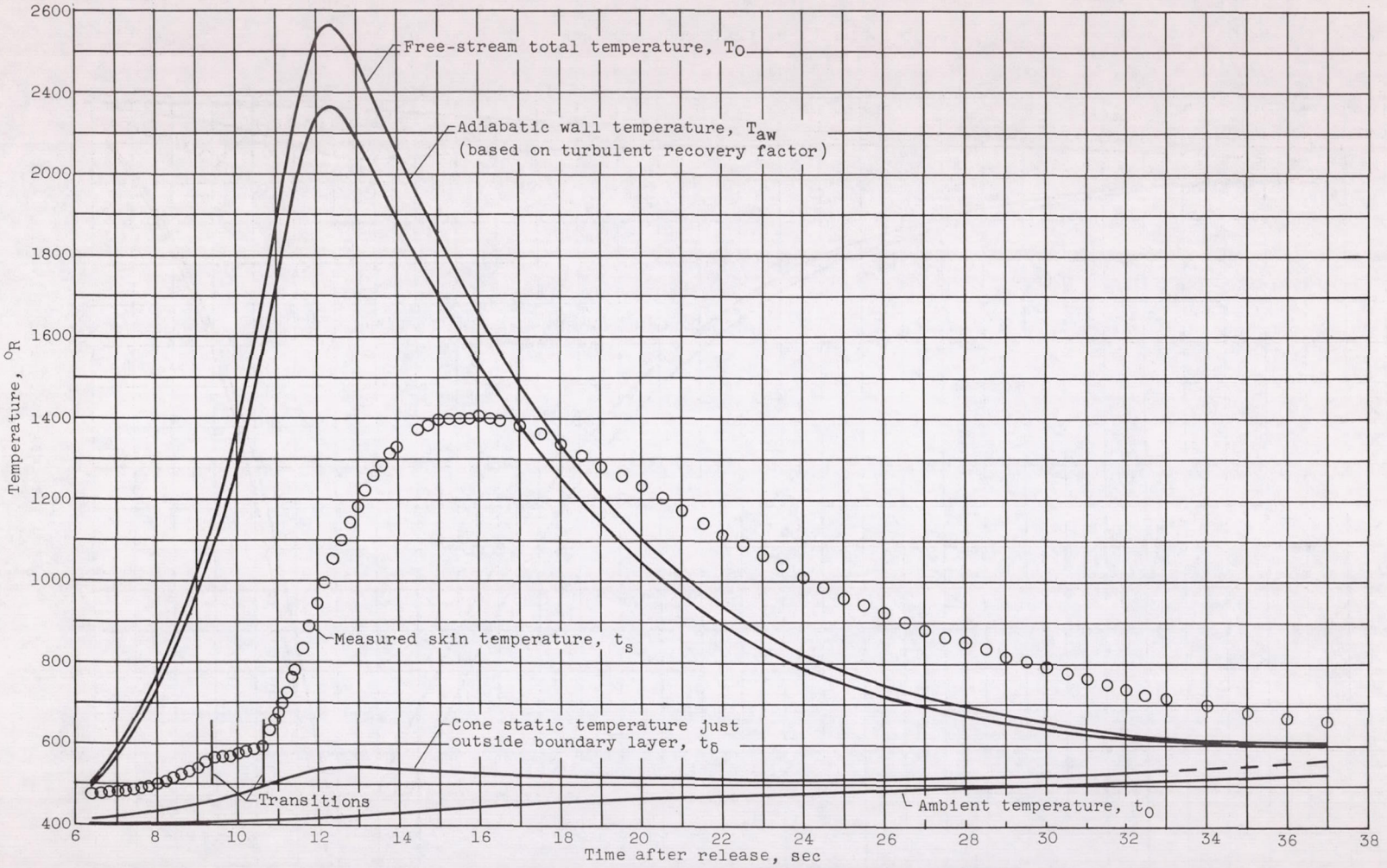

(f) Slant distance from cone apex, 25.84 inches.

Figure 8. - Continued. Time history of air and skin temperatures for 20-degree cone-cylinder test vehicle.

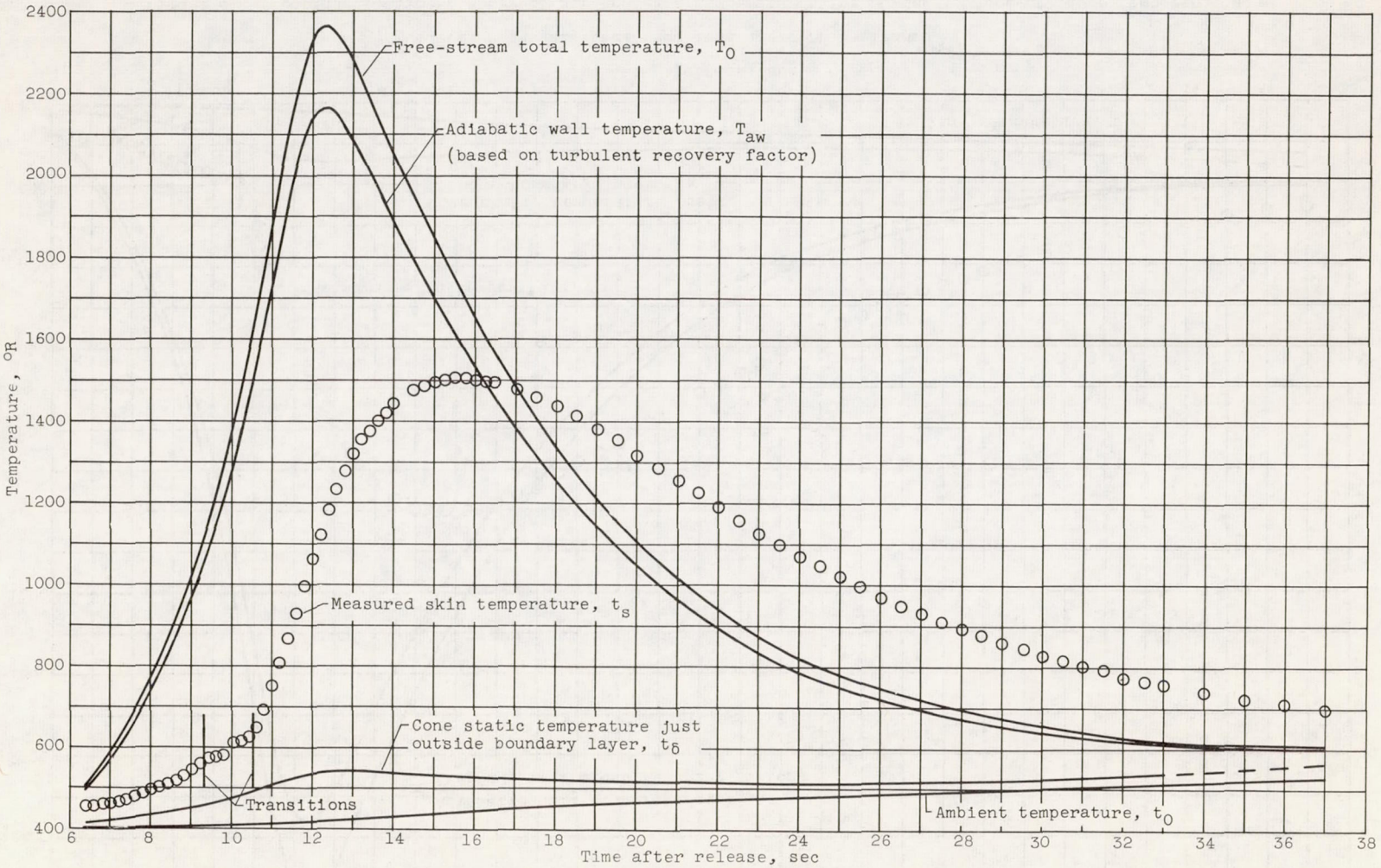

(g) Slant distance from cone apex, 23.53 inches; $\theta = 180^\circ$ (fig. 4).

Figure 8. - Concluded. Time history of air and skin temperatures for 20-degree cone-cylinder test vehicle.

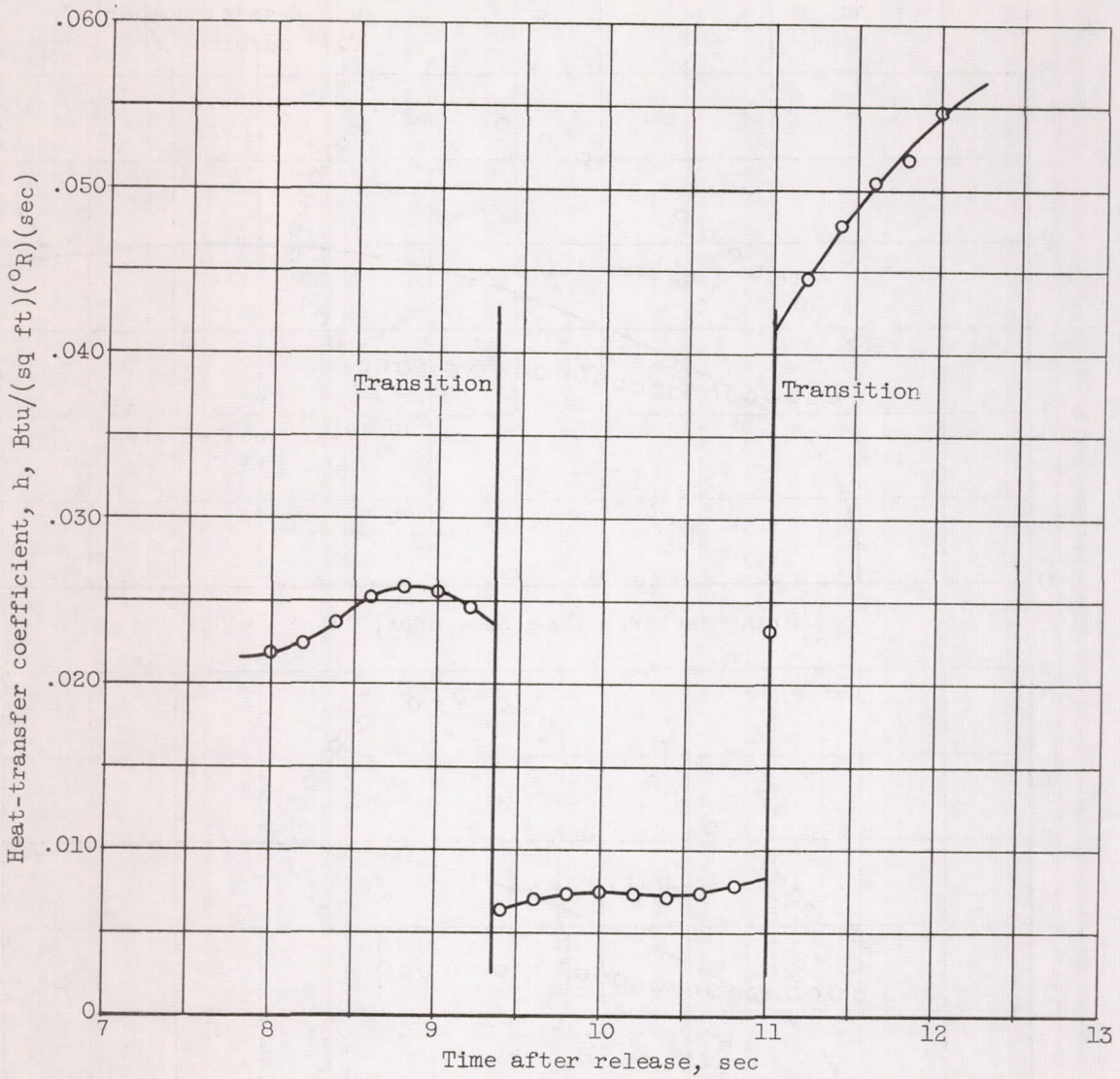

Figure 9. - Time history of heat-transfer coefficient at location 14.16 inches from tip during boundary-layer transition.

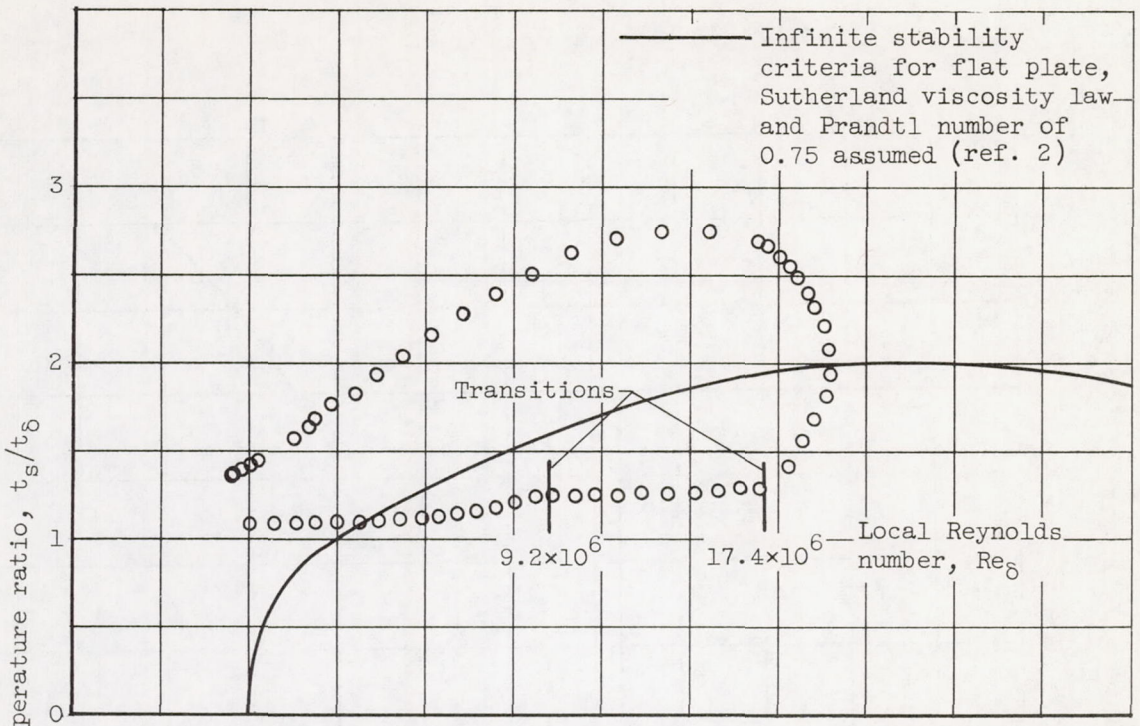

(a) Slant distance from cone apex, 11.66 inches.

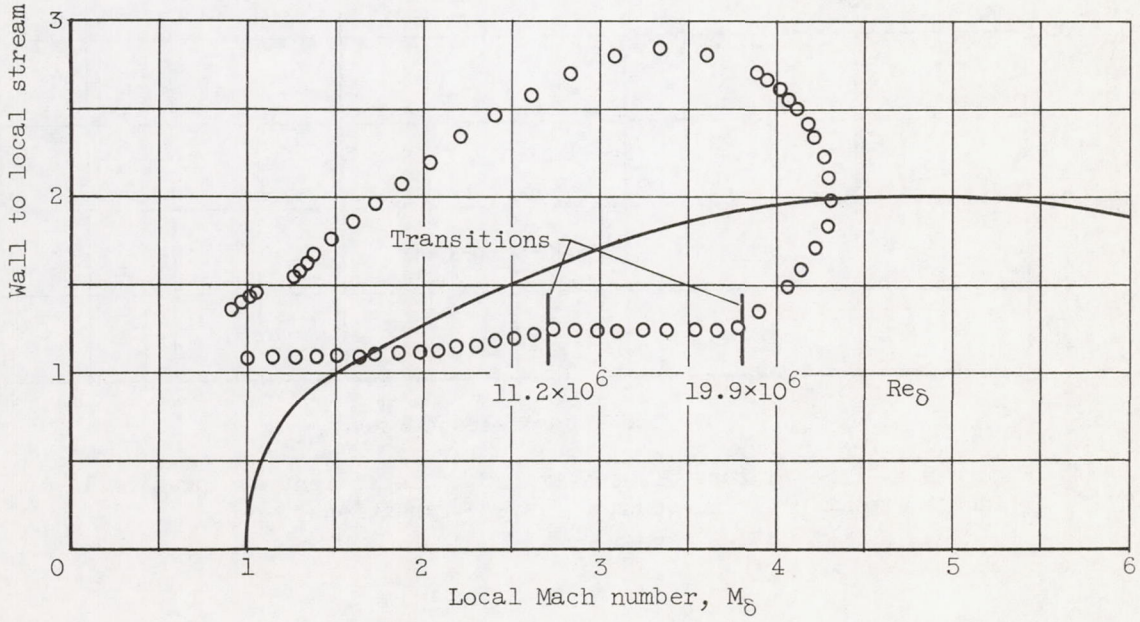

(b) Slant distance from cone apex, 14.16 inches.

Figure 10. - Variation of wall to local stream temperature ratio with local Mach number.

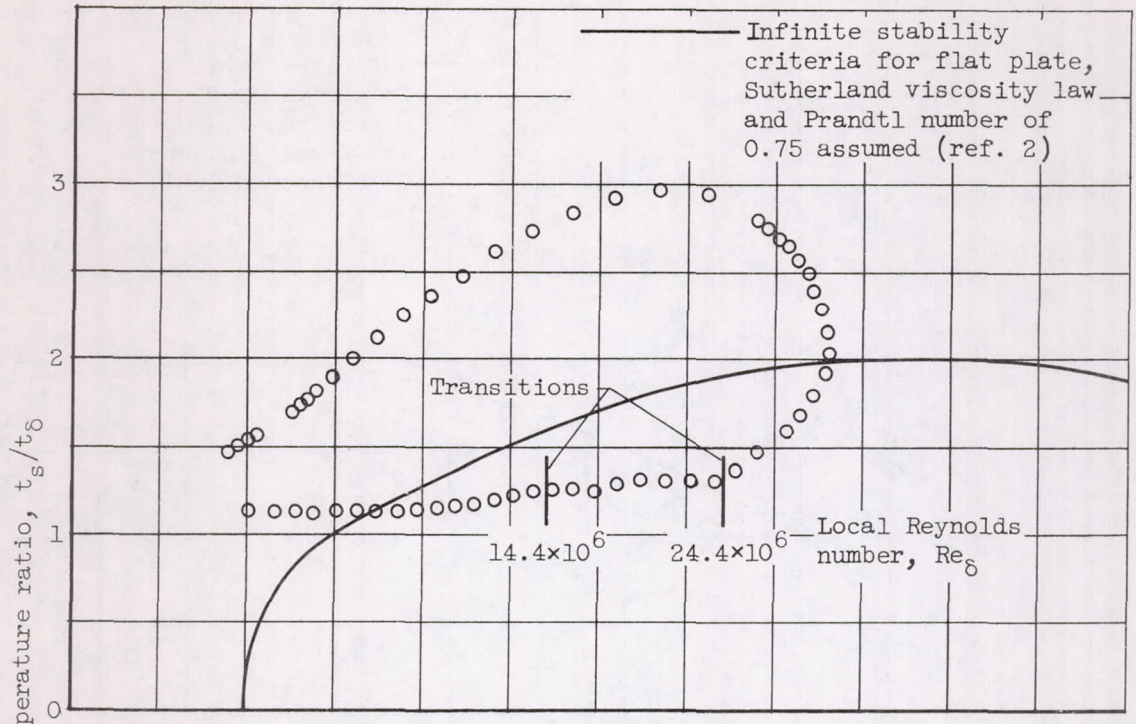

(c) Slant distance from cone apex, 18.28 inches.

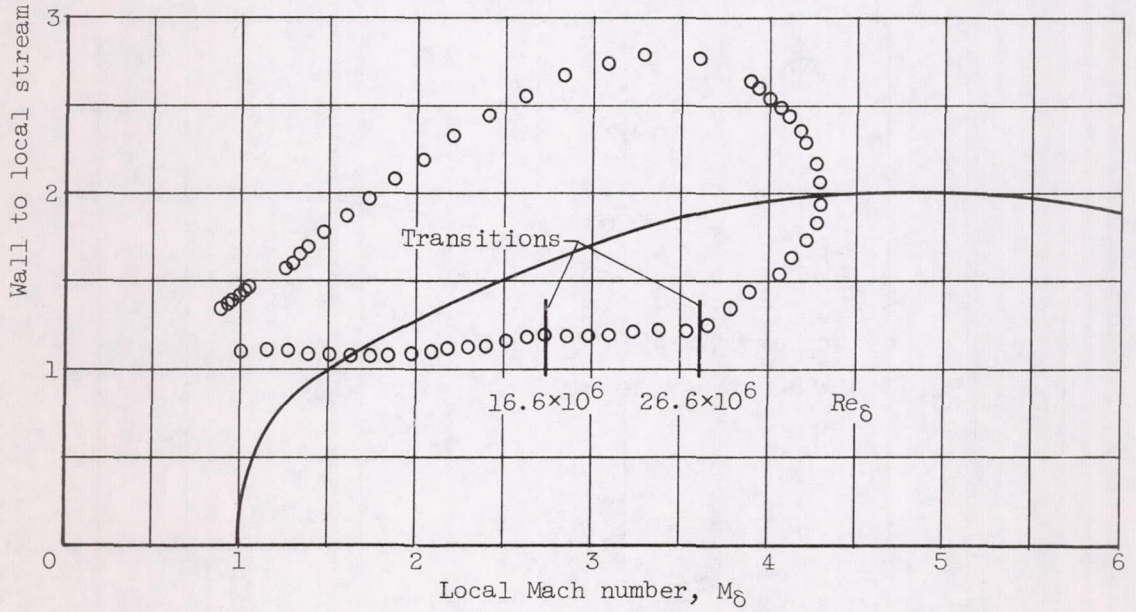

(d) Slant distance from cone apex, 20.97 inches.

Figure 10. - Continued. Variation of wall to local stream temperature ratio with local Mach number.

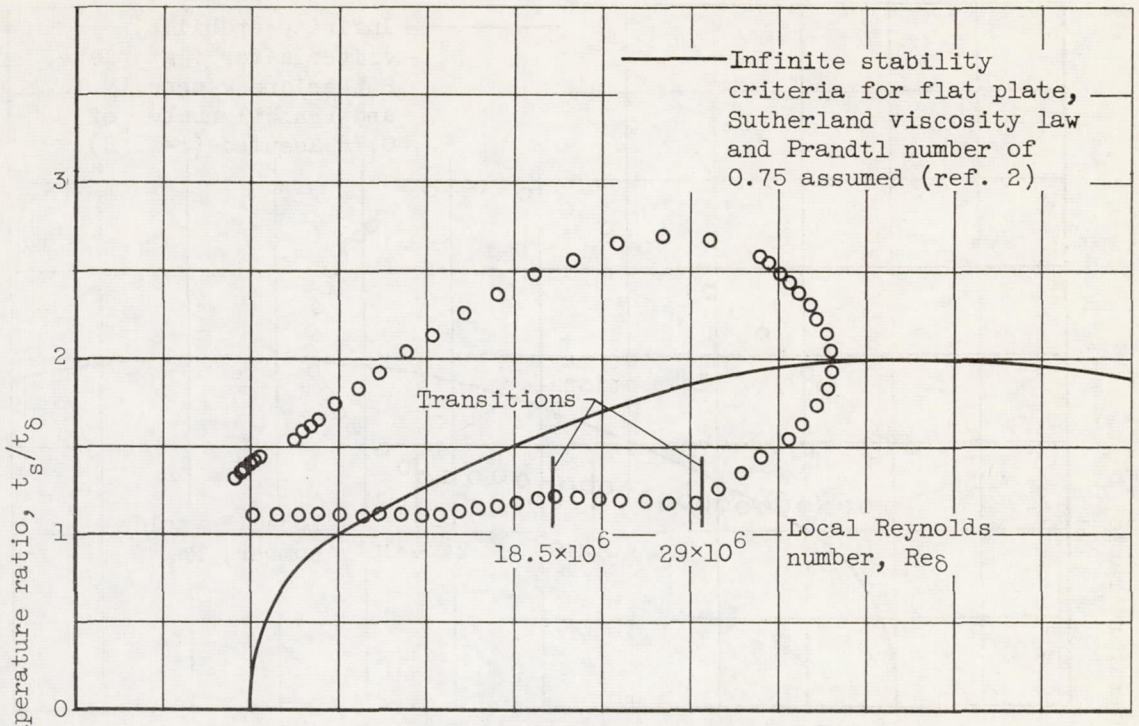

(e) Slant distance from cone apex, 23.53 inches.

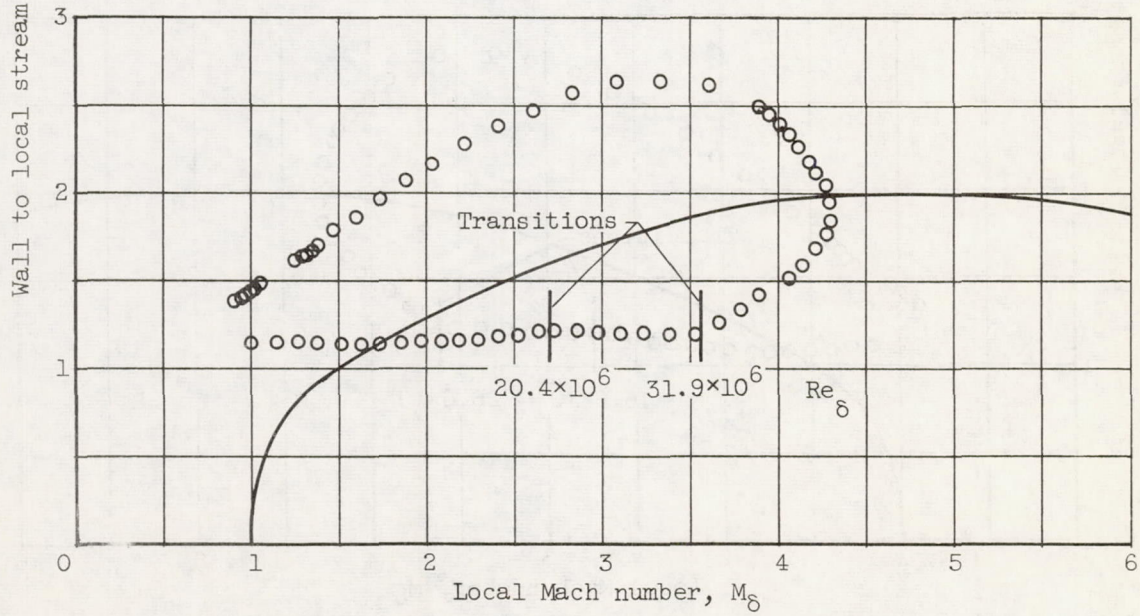

(f) Slant distance from cone apex, 25.84 inches.

Figure 10. - Continued. Variation of wall to local stream temperature ratio with local Mach number.

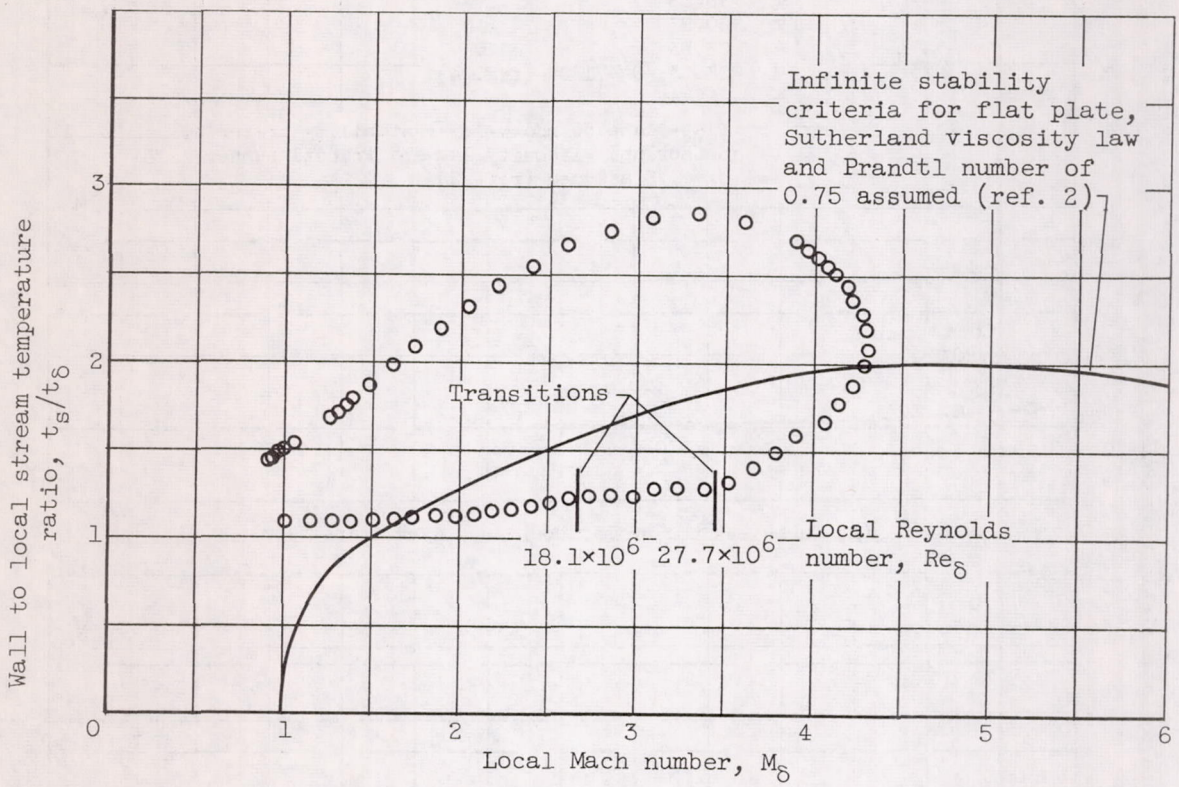

(g) Slant distance from cone apex, 23.53 inches; $\theta = 180^{\circ}$ (fig. 4).

Figure 10. - Concluded. Variation of wall to local stream temperature ratio with local Mach number.

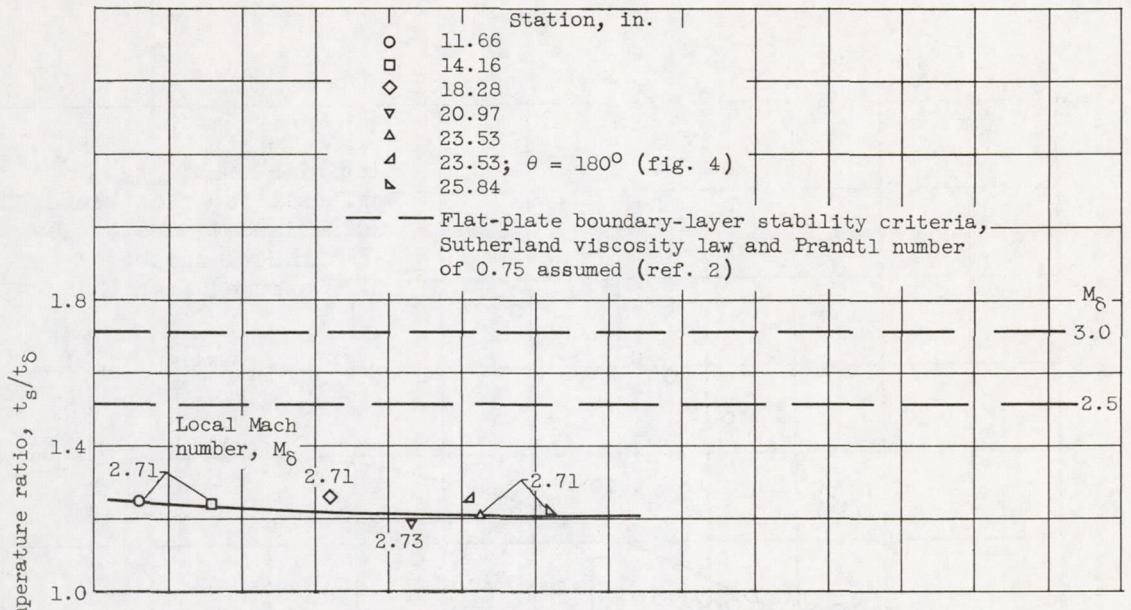

(a) Turbulent to laminar boundary-layer transition.

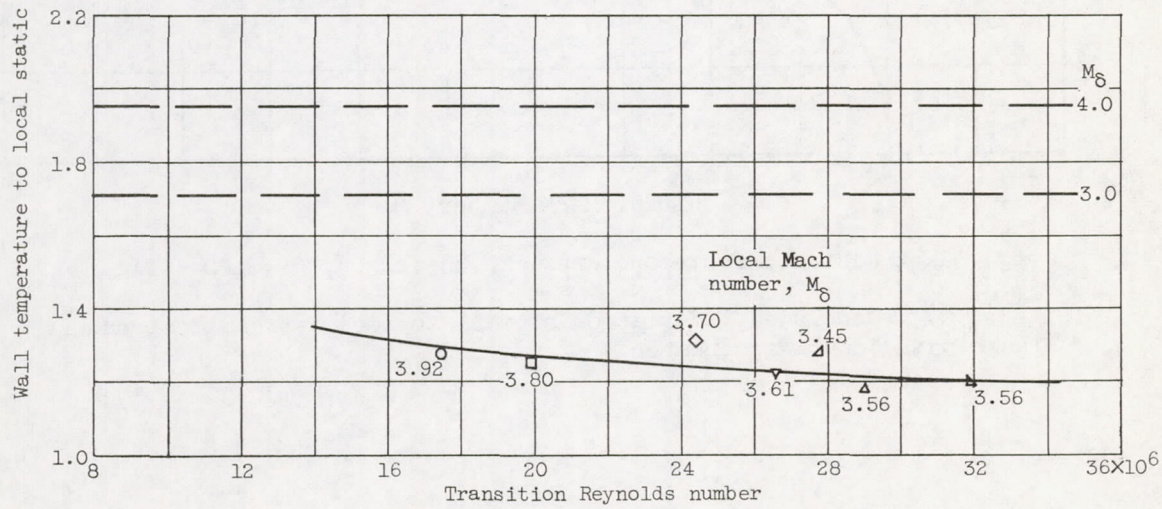

(b) Laminar to turbulent boundary-layer transition.

Figure 11. - Variation of wall to local stream temperature ratio with transition Reynolds number.

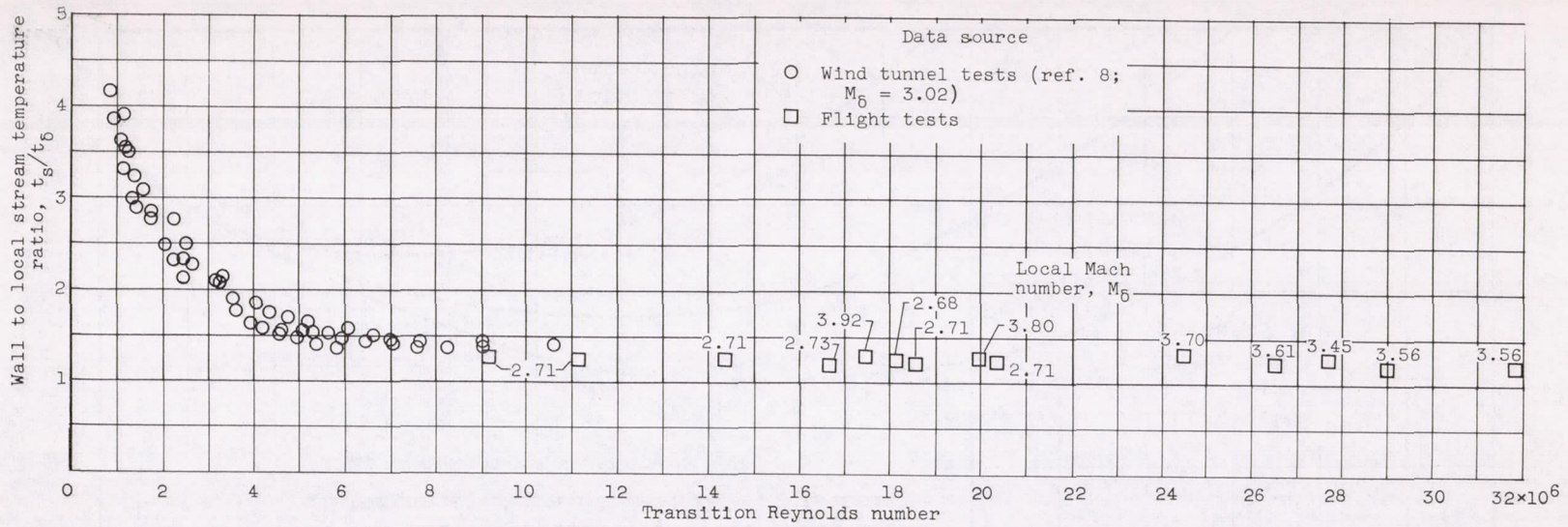

Figure 12. - Comparison of flight and wind tunnel boundary-layer transition data.

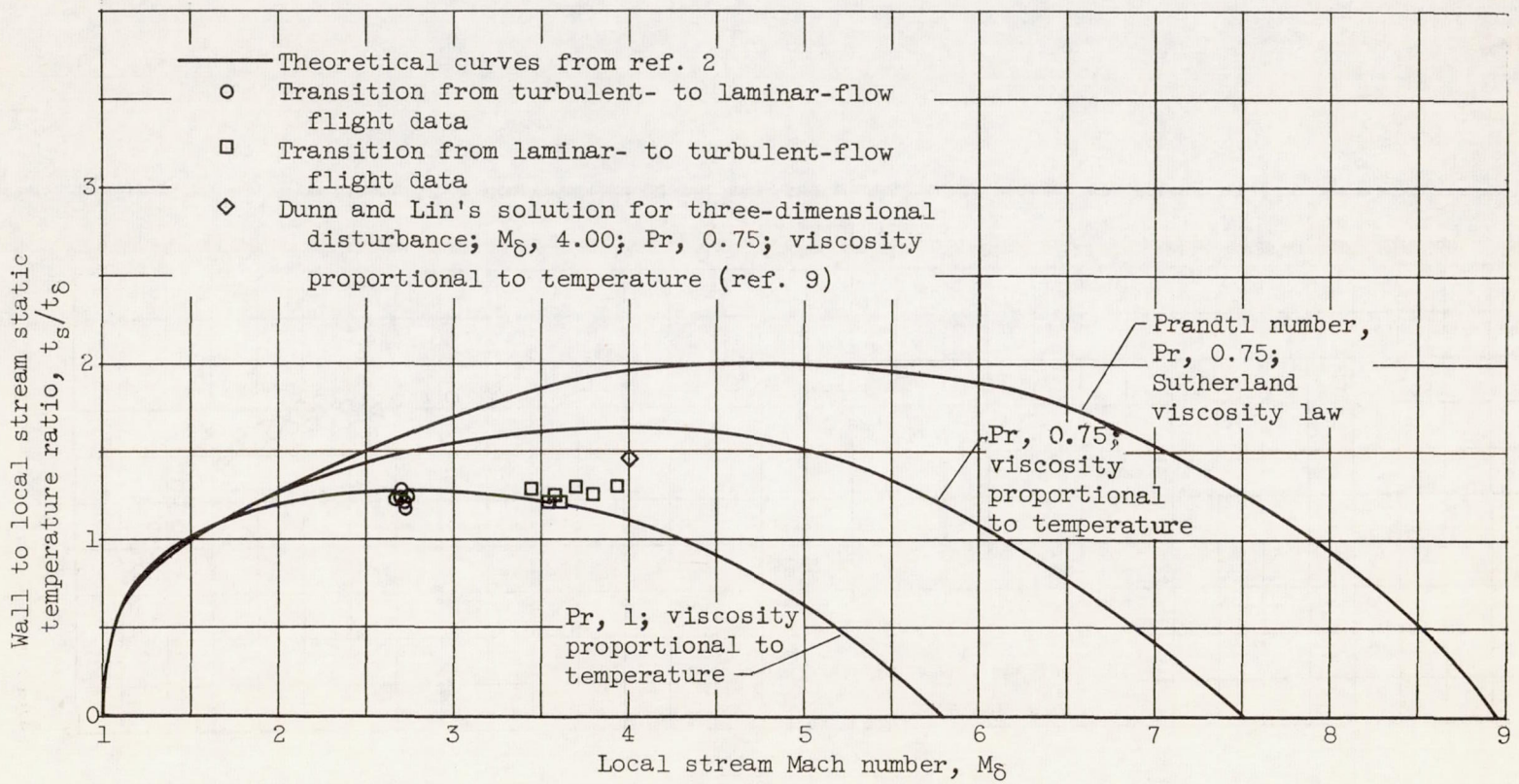

Figure 13. - Comparison of boundary-layer transition data from free-flight tests with several theoretical solutions for boundary-layer stability criteria at infinite Reynolds number (refs. 2 and 9).

NACA - Langley Field, Va.